Yuzuncu Yil University Journal of the Institute of Natural & Applied Sciences, Volume 28, Issue 2 (August), 591-619, 2023

Yuzuncu Yil University
Journal of the Institute of Natural & Applied Sciences
https://dergipark.org.tr/en/pub/yyufbed

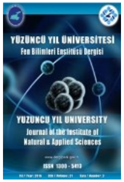

Research Article

Characterization of Polymeric Wastes in the Hygienic Product Factory and Energy Recovery from These Wastes

Hatice KELEŞ[1], Yunus ÖNAL[*2], Yeliz AKBULUT[2]

[1]Eruslu Global Group of Companies, 4th Industrial Zone, 83424 Street, No: 3-5, Şehitkamil, 27630, Gaziantep, Türkiye
[2]Inonu University, Engineering Faculty, Chemical Engineering Department, 44280, Malatya, Türkiye
Hatice KELEŞ, ORCID No: 0000-0002-6762-3929, Yunus ÖNAL, ORCID No: 0000-0001-6342-6816, Yeliz AKBULUT, ORCID No: 0000-0002-0703-7055
*Corresponding author e-mail: yunus.onal@inonu.edu.tr

Article Info

Received: 15.09.2022
Accepted: 27.02.2023
Online August 2023

DOI:10.53433/yyufbed.1174707

Keywords
FT-IR,
Polymer characterization,
TGA-DTA,
Waste polymer

Abstract: In this study, the characterization of polymeric wastes released during production in Eruslu Global group companies and the re-evaluability of these wastes were studied. For this purpose, all polymeric wastes that occur in the production of sanitary napkins, diapers, packaging film and printed packaging film, which are the basic production products of the enterprise; It was determined that it consists of polypropylene, polyethylene (LDPE, MDPE, HDPE), polystyrene, polyethylene terephthalate polymers. Considering that all wastes are not polluted, it has been evaluated that they can be reused to a large extent. In the study conducted for this purpose, it was determined that 20 different waste products emerged depending on the product variety produced in the enterprise. Thermal analysis for each waste was characterized by calorific value, FTIR, XRD, SEM and TG-DSC (TGA-DTA) techniques. It was determined that paint was added to polymeric wastes in general. In addition, it has been determined that natural micronized calcite is added to some waste in terms of environmental impact and cost reduction. This article evaluates the crystallinity, structure and surface morphology of polymeric wastes produced during production in Eruslu Global group companies. For this purpose, all polymeric waste products formed in the production of sanitary napkin, diapers, packaging film and printed packaging film, which are the primary production products of the enterprise, were characterized. 20 different waste products produced in the enterprise were selected for evaluation. Waste is rich in polystyrene, polypropylene, polyethylene (LDPE, MDPE, HDPE) and polyethylene terephthalate polymers. Each waste was characterized by FTIR, XRD, SEM, thermal analysis and calorific value techniques. As a result of the study, dye additive was detected in the structure of these wastes. When the XRD results were evaluated, it was determined that micronized calcite was added to the polymers to prevent environmental pollution caused by the paint additive. In this way, environmental pollution and production costs are reduced. Calorific values of all samples are in the range of 4292 - 10965 cal/g.

Hijyenik Ürün Fabrikasında Oluşan Polimerik Atıkların Karakterizasyonu ve Bu Atıklardan Enerji Geri Kazanımı

Makale Bilgileri

Geliş: 15.09.2022
Kabul: 27.02.2023
Online Ağustos 2023

Öz: Bu çalışmada Eruslu Global grup şirketlerinde üretim sırasında açığa çıkan polimerik atıkların karakterizasyonu gerçekleştirilmiş ve bu atıkların yeniden değerlendirilebilirliği araştırılmıştır. Bu amaçla işletmenin temel üretim ürünlerinden kadın pedi, çocuk bezi, ambalaj filmi ve baskılı ambalaj filmi üretiminde meydana gelen tüm polimerik atıkların; polipropilen, polietilen

DOI:10.53433/yyufbed.1174707

(LDPE, MDPE, HDPE), polistiren, polietilen tereftalat polimerlerinden oluştuğu belirlenmiştir. Tüm atıkların kirlenmediği göz önüne alındığında büyük oranda yeniden kullanılabileceği değerlendirilmiştir. Bu amaçla yapılan çalışmada işletmede üretilen ürün çeşitliliğine bağlı olarak 20 farklı atık ürün ortaya çıktığı belirlenmiştir. Her bir atık için termal analiz, ısıl değer, FTIR, XRD ve SEM teknikleri ile karakterize edilmiştir. Polimerik atıklara genel olarak boya katkılandığı belirlenmiştir. Ayrıca çevresel etki açısından ve maliyet düşürücü olarak bazı atıklarda doğal mikronize kalsit katıldığı belirlenmiştir. Bu makalede, Eruslu Global grup şirketlerinde üretim sırasında oluşan polimerik atıkların kristalliği, yapısı ve yüzey morfolojisi değerlendirilmektedir. Bu amaçla işletmenin birincil üretim ürünleri olan hijyenik kadın pedi, çocuk bezi, ambalaj filmi ve baskılı ambalaj filmi üretiminde oluşan tüm polimerik atık ürünler karakterize edilmiştir. İşletmede üretilen 20 farklı atık ürün değerlendirilmek üzere seçilmiştir. Atık, polistiren, polipropilen, polietilen (LDPE, MDPE, HDPE) ve polietilen tereftalat polimerleri açısından zengindir. Her bir atık, FTIR, XRD, SEM, termal analiz ve ısıl değer teknikleri ile karakterize edilmiştir. Çalışma sonucunda bu atıkların yapısında boyar madde katkısı tespit edildi. XRD sonuçları değerlendirildiğinde, boya katkı maddesinin neden olduğu çevre kirliliğini önlemek için polimerlere mikronize kalsit ilave edildiği belirlendi. Bu sayede çevre kirliliği ve üretim maliyetleri azaltılmaktadır. Tüm numunelerin kalorifik değerleri 4292 - 10965 cal/g aralığındadır.

Anahtar Kelimeler
Atık polimer,
FT-IR,
Polimer karakterizasyon,
TGA-DTA

1. Introduction

Polymeric products are widely used in all areas of human life, especially in housing, food, medicine, and chemistry (Guyot & Bartholin, 1982). The amounts and compositions of polymer wastes have increased day by day as technology has advanced. Today, important industrial chemical processes such as OXO, Fischer-Tropsch, and Sasol use polymeric wastes as raw materials. The most important advantage of this use will be to include polymeric wastes in the global carbon cycle. Türkiye has a solid waste plastics rate of 5-14%. These plastics are classified as thermoplastics and thermosets (Tayyar & Üstün, 2010; Hejna et al., 2020; Durga et al., 2021; Phakedi et al., 2021; Srinivasan et al., 2021; Yuan et al., 2021). Thermoplastics include Polystyrene (PS), Polypropylene (PP), Polyethylene (PE), Polyvinyl Chloride (PVC), and Polyethylene Terephthalate (PET). These widely used thermoplastics can be re-evaluated using chemical recycling energy recovery, and mechanical recycling methods (Paci & La Mantia, 1999; Khadzhiev et al., 2016; Costa et al., 2019; Pan et al., 2021; Siwal et al., 2021). There are four different approaches for recyclable polymeric/plastic waste. These approaches are primary recycling, secondary recycling, tertiary recycling, and quaternary recycling (Ignatyev et al., 2014; Francis, 2016; Singh et al., 2017; Zhuang et al., 2022). Primary recycling is carried out by adding waste to the fresh raw material at a certain rate during production. Secondary recycling is the use of waste by mixing it with other polymers. This method, also referred to as "mechanical recycling," includes physical processes such as separation, grinding, melting, and reshaping. Waste polymer can be reprocessed by melt extrusion. In tertiary recycling, wastes are broken down (solvolysis) in the presence of various solvents by chemical reactions, and thus the obtained raw products can be reused in production (Kumar, 2021). It is also called chemical recycling. Decomposition can also be achieved by thermal decomposition (pyrolysis) in an oxygen-free environment. In the last method, which is expressed as "quaternary recycling" or "energy recovery," the energy content of the wastes is recovered by burning (da Silva & Wiebeck, 2020). Pyrolysis (controlled combustion in a nitrogen atmosphere) is one of the chemical recycle techniques. This technique is frequently used to produce valuable chemicals with high yields. With the pyrolysis technique, the excess amount of waste, waste disposal, and environmental pollution that pose a problem are eliminated. Thus, renewables, eco-innovation and fossil resource use in the traditional plastics industry are improved (Picuno et al., 2020). The efficiency of solids, liquids and gases, which are products of the pyrolysis technique, can be increased. There are studies that increase the product yield depending on the type of polymer and the catalyst used (Padhan & Gupta, 2018). One article studied the recycling of PET bottles and PE bags, which are major plastic pollutants. The obtained results were shared in the literature (Rajasekaran & Maji, 2018). In another article, a new composite material was produced using polyethylene terephthalate bottle waste and marble dust. The thermal and mechanical properties of the newly manufactured composite material were investigated (Çınar & Kar, 2018). In another article, chemical recycling of LDPE, HDPE and PP was investigated using two different methods (Achilias et al., 2008). In another article, the recycling of polymers by mechanical and chemical methods was investigated (Ragaert et al., 2017). In another paper, they investigated the usability of major thermoplastic polymers to obtain recyclable materials in a variety of industrial and indoor applications. The density, mechanical resistance, design and chemical properties of the produced materials have been improved. They worked on the recycling of thermoplastic polymers and the development of recycling technology (Grigore, 2017). Issues such as recycling of waste polymers, incineration technologies and energy generation have been extensively studied in the literature (Ramarad et al., 2015; Bahoria et al., 2018; Padhan & Gupta, 2018; Saleem et al., 2018). Recycling plastic and polymer wastes to make them reusable provides a significant economic gain. On the other hand, it will play an important role in the protection of natural resources. Many studies have been carried out in the literature for the recycling of waste polymers and the application of recycling methods (Baechler et al., 2013; Okan et al., 2019). In addition, there are many articles on the physical, structural and mechanical properties of recycling products (Hamad et al., 2013; Valerio et al., 2020). In the literature, there are many studies on the characterization of recycling products made from polyethylene, polypropylene, polystyrene and polyethylene terephthalate materials, which are widely used industrially (Achilias et al., 2007; Al-Salem et al., 2009; Ghosal & Nayak, 2022; Hamad et al., 2013; Suhaimi et al., 2022). This study evaluating Eruslu Health Group wastes was a pilot study that will shed light on the importance of waste management, characterization, recycling, and energy recovery. The aim of this article is to characterize Eruslu Group waste polymer products by calorific value, TGA-DTA, FTIR, XRD, and SEM methods and contribute to the literature on waste polymer characterization.

2. Material and Methods

Eruslu Global Group of Companies was established in 1996. This company produces in the chemical, textile, construction, packaging, and hygiene sectors. In 2004, it started to produce diapers under the Sleepy brand. It produces products such as adult patient diapers, sanitary napkins, wet towels, and napkins belonging to the Sleepy brand. In this study, 20 different polymer wastes from Sleepy were used as raw materials. The wastes were dried in an oven at 105°C. The dried wastes were characterized by calorific value, FT-IR, XRD, SEM and TGA-DTA methods.

2.1. Material

In this study, waste polymeric materials released as waste in Eruslu Global Company were used (Akdağ, 2019). Waste polymers were directly characterized without chemical pretreatment.

Abbreviations and polymer types of waste polymers are given in Table 1.

Table 1. Names, types and codes of waste polymers

Example	Polymer Type	Code
Exterior Cladding (Foam)	Polystyrene (PS)	1
Eco Raw Material Bag (Outside Aluminum)	Polyethylene (PE)	2
Green Cliche Tape	Polyethylene Terephthalate, Polyethylene (PET+PE)	3
Orange Cliche Tape	Polyethylene Terephthalate, Polyethylene (PET+PE)	4
Fiber Powder	Polyethylene Terephthalate (PET)	5
Sack Circle	Polypropylene (PP)	6
Waste Spunlace Fabric	Polyethylene Terephthalate (PET)	7
Bz Raw Material Bag	Polypropylene, Kraft paper (PP+Kraft paper)	8
C Band Wedge	Polyethylene, Polyethylene Terephthalate, Synthetic Rubber	9
Dirty Cloth	Polyethylene Terephthalate (PET)	10

Table 1. Names, types and codes of waste polymers (continued)

Example	**Polymer Type**	**Code**
Oily Cloth	Polyethylene Terephthalate (PET)	11
Green Adl Sample	Polyethylene Terephthalate (PET)	12
C Band Sample	Polyethylene, Polyethylene Terephthalate, Synthetic Rubber	13
Flexible Ear Sample	Polypropylene (PP)	14
White Adl Sample	Polyethylene Terephthalate (PET)	15
Tbs Sample	Polypropylene, Polyethylene Terephthalate, Synthetic Rubber	16
Mini Sideband Sample	Polypropylene, Synthetic Rubber	17
Sbs Sample	Polyethylene, Polyethylene Terephthalate, Synthetic Rubber	18
Barrier Sample	Polypropylene (PP)	19
Tissue Sample	Polypropylene (PP)	20

The wastes listed in Table 1 are shown in Figure 1, respectively.


(1) (2) (3) (4) (5)
(6) (7) (8) (9) (10)
(11) (12) (13) (14) (15)
(16) (17) (18) (19) (20)

Figure 1. Images and codes of waste polymers.

2.2. Characterization of waste polymers

SEM analyzes were performed with the “LEO-EVO 40/Cambridge-England” brand device in the central research laboratory of Inonu University. Electron acceleration and generation mechanisms in the analyzes were carried out with the traditional method. XRD analyzes are Rigaku RadB-Dmax II and Rigaku RINT-2000 X-ray diffractometers available at the Inonu University scientific research center (IBTAM). There is also a Jade 6 + crystal analysis program and library integrated into these systems. In the analysis, the electromagnetic beam of a certain wavelength was reflected by hitting the material surface and the reflected beam was interpreted according to Bragg's Law. FTIR analyses of the samples were performed with PerkinElmer Spectrum One device in the Central Research Laboratory of Inonu University in the range of 500–4000 cm^{-1}. Thermal analyzes were made with Shimadzu brand TA 50 model and DTA 50 model thermal analyzers. The calorific value analysis was made with the PARR 1341 Plain Jacket Calorimeter.

2.2.1. Calorific value analysis

Heating values of waste polymers were calculated with the following formula (Equation 1 and 2).

$$HHV = \frac{(\Delta t * W) - e * 2.3}{W} \tag{1}$$

$$LHV = 1.8 * HHV - 91.23 * H \tag{2}$$

where, HHV: Higher heating value (cal/g), LHV: Lower heating value (cal/g), Δt : Change of temperature (t_2 –t_1) (°C), t_2 : final temperature, t_1 : initial temperature, W: mass of the sample used, E : length of wire and H is the hydrogen content of the sample.

0.5 grams of waste polymers were weighed for calorific value analysis. It is built into the calorimeter bomb in the cuvette. Wire was used as a burning apparatus. Combustion was carried out in the presence of 25 atm of oxygen. Then the upper and lower calorific values were calculated.

Figure 2. Image of Series 1341 plain jacket oxygen combustion calorimeters.

3. Results

3.1. FT-IR analysis results

FTIR spectra of polymer samples with waste PE structure are given in Figure 3. The FTIR spectra of the samples are similar according to the polymers they contain. For the added inorganic components, the peak area changes depending on the amount.

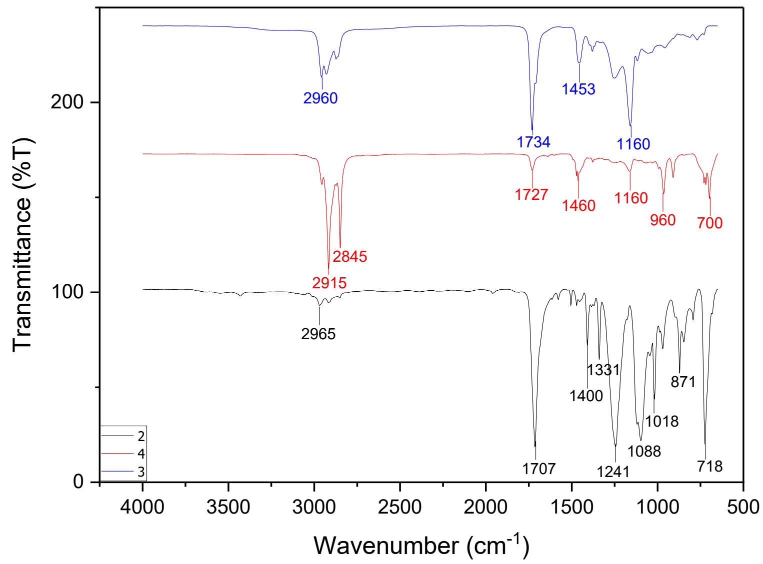

Figure 3. FTIR spectrum of wastes belonging to eco raw material bag, orange plate tape and green plate tape.

Table 2. FTIR spectrum and ash evaluation (Asgari et al., 2014)

Sample	**Ash (%)**	**Peak (cm^{-1})**	**Group**
Eco Raw Material Bag	16.33	2 900	Aliphatic C-H (Campbell et al., 2000)
Green Cliche Band	0.68	1 407, 871 and 718	Calcite and aragonite (Özsin et al., 2020)
Orange Cliche Band	6.45	2 900, 1 752	Aliphatic C-H, C=O (El-Saftawy et al., 2014)

The change in the peak intensities according to the polymer inorganic additive ratios is clearly seen.

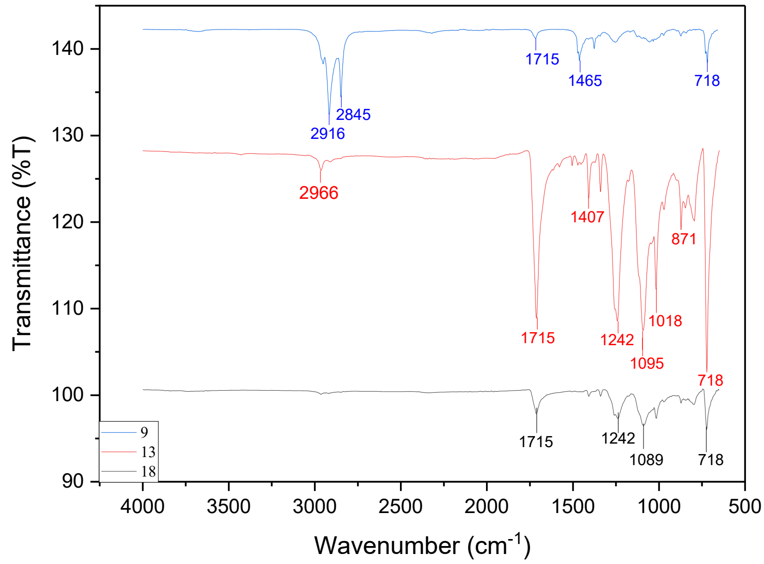

Figure 4. FTIR spectrum of wastes from C Band wedge, C band sample and SBS sample.

Table 3. FTIR spectrum and ash evaluation (Kaur et al., 2023)

Sample	Ash (%)	Peak (cm^{-1})	Group
C-Band wedge	0.74	2 916, 1 715	Aliphatic C-H, C=O (Campbell et al., 2000)
C-band sample	0.25	1 407, 871 and 718	Calcite (Özsin & Pütün, 2018)
SBS Sample	1.61	1 715	C=O (Achilias et al., 2007)

The PE ratio of the C-Band wedge is high. The mixture of rubber and PE prevented PET bands from appearing prominently in the FTIR spectrum. The low PET ratio was also effective in this. SBS Sample mainly contains synthetic rubber. In addition, it contains low percentage of PET and PE. Since the PE ratio is low, the aliphatic C-H stretch is in the form of a very weak peak. The calcite contribution in this waste is lower than the others.

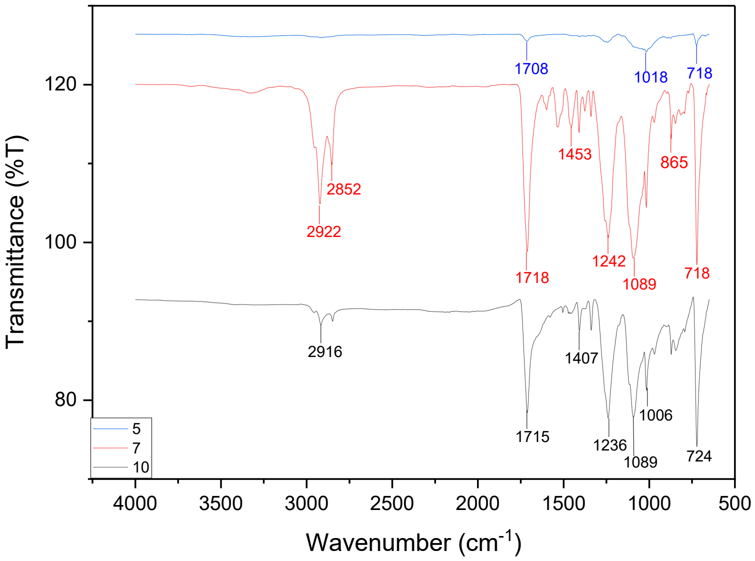

Figure 5. FTIR spectrum of fiber dust, waste spunlace fabric and soiled cloth.

Table 4. FTIR spectrum and ash evaluation (Tonetto et al., 2013)

Sample	Ash (%)	Peak (cm^{-1})	Group
Fiber Powder	0.74	1 708, 1 018	C=O (Gulmine et al., 2002)
Waste Spunlace Fabric	0.62	2 922, 2 852, 1 718, 1 453, 1 242, 1 089	Aliphatic and Aromatic C-H, C=O (Caro & Comas, 2017)
Dirty Cloth	2.54	2 916, 1 715, 1 407, 1 236, 1 089, 1 006	C=O, Calcite (Barrios et al., 2012)

Figure 5 calcite, 718 cm^{-1} peak of pure PET fiber powder is weakly visible. Waste Spunlace fabric is a typical FTIR spectrum of PET. The broad band of 3 089 - 3 533 cm^{-1} in the spectrum of the waste spunlace fabric belongs to the -OH stretch in water absorbed by PET. The peak around 1 242 cm^{-1} belongs to the vibration of the ester group. 1 453, 824 and 718 cm^{-1} peaks indicate that the sample in question contains calcite. Dirty cloth is in PET structure and belongs to the vibration of 1 715 cm^{-1}, aliphatic and aromatic C-H stresses in its structure. The 1 713 cm^{-1} peak belongs to the -C=O (carbonyl) stretch specific to the carboxyl groups. Dirty cloth is used in the factory environment for cleaning daily machines and the environment.

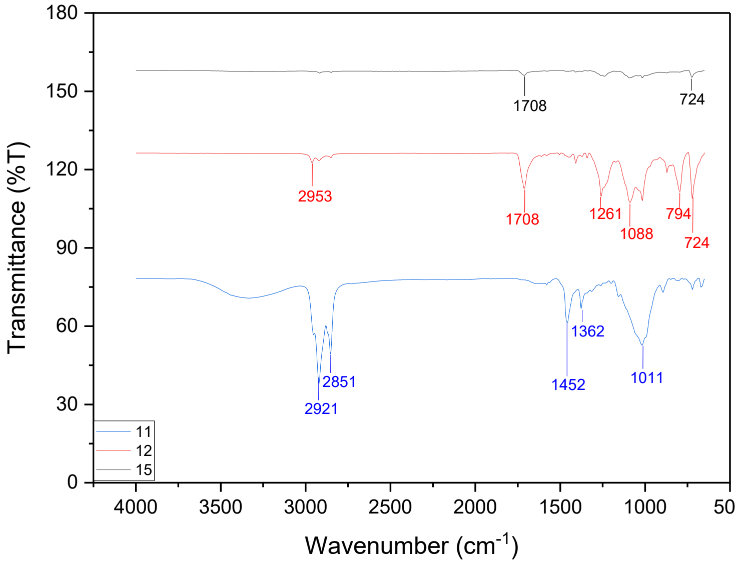

Figure 6. FTIR spectrum of oily cloth, green adl sample and white adl sample.

When Figure 6 is examined, the peaks of the oily cloth sample are quite weak. Although the green adl sample and the white adl sample have the same content, the spectra differ. The green adl sample contains dye. The white adl sample is in pure PET structure. The broad band 3 089-3 533 cm^{-1} in the white adl sample belongs to the -OH stretch of water. This band shows that the PET sample binds water with hydrogen bond.

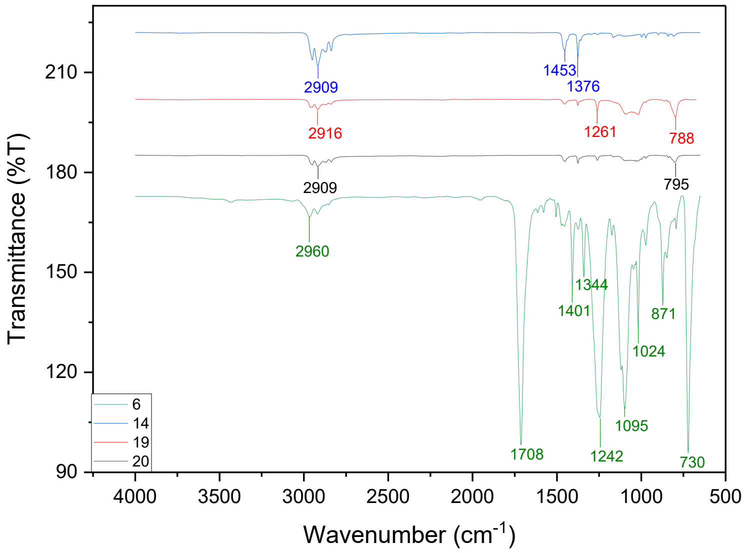

Figure 7. FTIR spectrum of sack circle, flexible flap, barrier sample and tissue sample.

Table 5. FTIR spectrum and ash evaluation (Riaz & Ashraf, 2014)

Sample	Ash (%)	Peak (cm^{-1})	Group
Sack Circle	0.05	1 708	C=O (Chalmers & Everall, 1999)

When Figure 7 is examined, peaks of aliphatic C-H stretching are seen in the Sack Circle. The Flexible Ear material made of polypropylene is the flexible parts on the sides of the diaper, the barrier sample serves to prevent the liquid from coming out on the sides, the tissue sample is the material that gives a soft feeling to the skin in the diaper. This part is the part that receives the liquid and transmits it to a substrate.

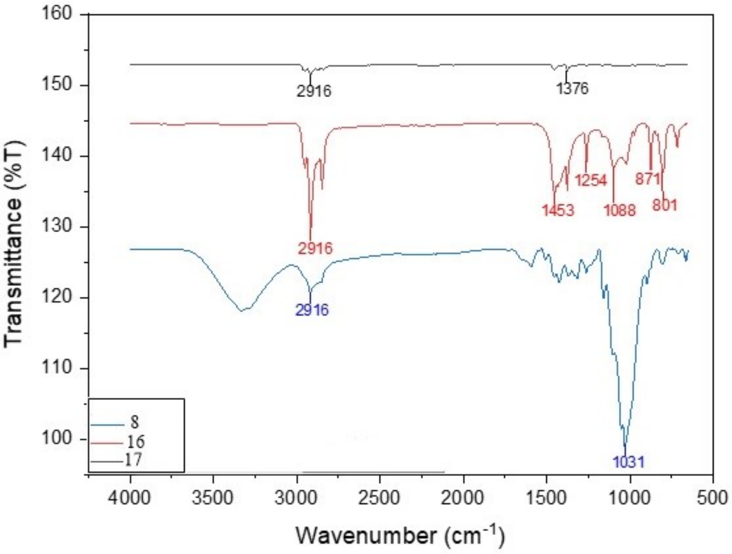

Figure 8. PP and other waste polymer FTIR graph.

Table 6. FTIR spectrum and ash evaluation (Kaur et al., 2023)

Sample	Ash (%)	Peak (cm^{-1})	Group
BZ Raw Material Bag	9.31	2 916, 1 031	Aliphatic C-H (Verdurmen-Noel et al., 2001)
TBS Sample	11.66	2 916, 1 453, 1 254	Aliphatic C-H (Fang et al., 2012)
Mini Sideband Sample	0.29	2 916, 1 376	Aliphatic C-H (Arutchelvi et al., 2008)

BZ Raw Material Bag Sample (PP-Kraft Paper) material is made of thick cardboard (Kraft) paper inner part is made of PP material. The peak with a peak minimum of 3 200 cm^{-1} belongs to the –OH stretch of water in cellulosic structure and hydrogen bonded. The 2 916 cm^{-1} peak belongs to the aliphatic C-H stretch in both cellulosic and PP structures. TBS Sample is a mixture of PP, PE and synthetic rubber. The aliphatic C-H stretch is seen as a sharp peak depending on all three materials in aliphatic structure. M-O peak around 1 000 cm^{-1} of the additive material calcite is clearly visible. The Mini Sideband sample contains only PP and synthetic rubber, and the aliphatic C-H stretch is clearly visible.

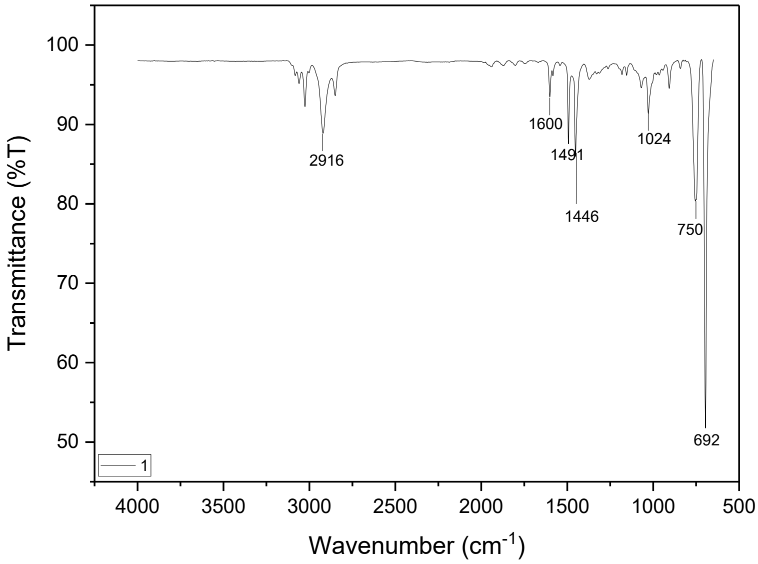

Figure 9. Facade ladding foam sample (PS) FTIR spectrum.

Exterior Cladding Foam Sample is polystyrene and is consistent with the literature. The peak around 3 000 cm^{-1} belongs to the aromatic C-H stretch (Campbell et al., 2000).

3.2. XRD analysis results

The XRD spectra of all waste polymer samples are given below. Since the additives such as inorganic calcite added to the polymeric material show a crystal structure, both the amorphous structure and the crystal structure of the additive are clearly seen in the XRD analysis.

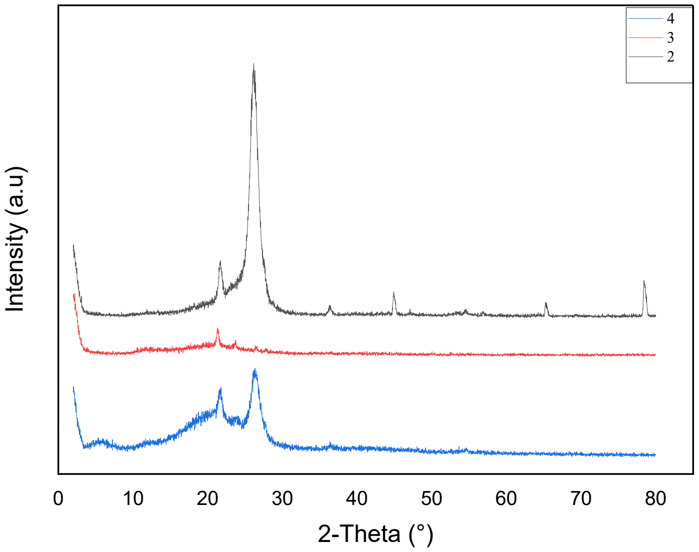

Figure 10. XRD graph of waste polymer in PE and PET+PE structure.

When the XRD spectrum of the Eco raw material sample made of PE is examined, the inner part is PE structure. The exterior is aluminum coated. The amorphous structure of PE is clearly visible. A crystalline structure peak is observed around 20 and 27 2θ depending on the aluminum on the outside. A semi-crystalline peak is observed around 22 and approximately 27 2θ of the orange cliché band (Tsai et al., 2015).

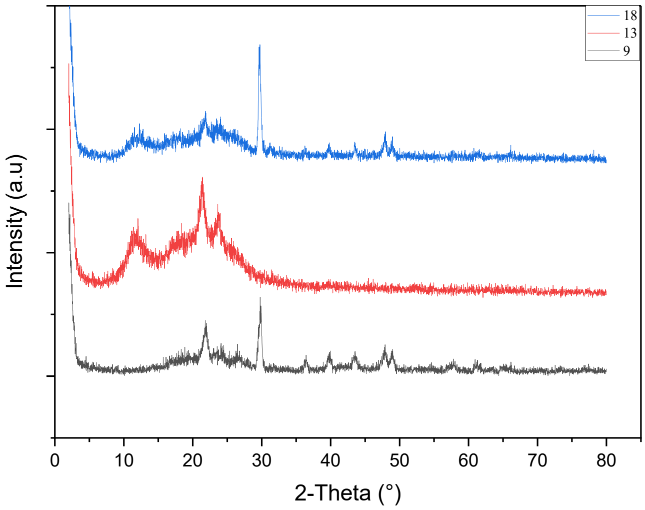

Figure 11. XRD graphic of waste polymer in PE+PET+Synthetic Rubber structure.

Both amorphous and crystalline structures are seen around 10 and 22 2θ of the C-band sample made of PET. The amorphous structure of the C-band wedge sample made of PET around 30 2θ is clearly visible. It is proved that it contains calcite with d=3.036 Å (Khanam & AlMaadeed, 2015).

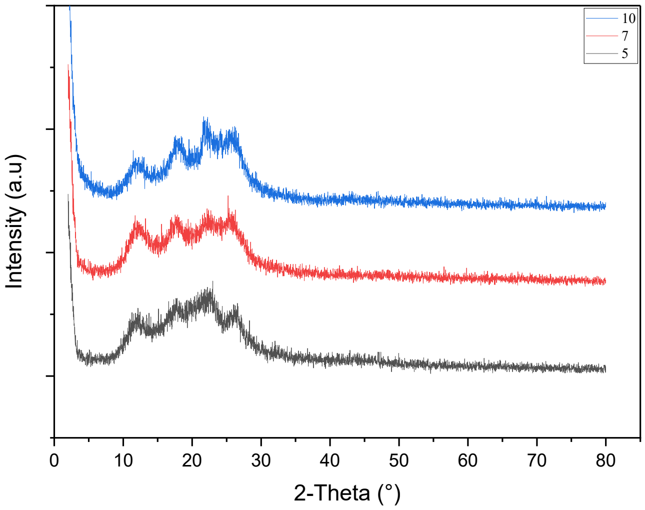

Figure 12. XRD graph of waste polymer in PET structure.

There are 3 peaks in amorphous structure around 20 2θ belonging to the dirty cloth (PET) sample. When the XRD of the waste spunlace sample made of PET is examined, it shows structural similarity with wet wipes. The inorganic additive content is very low (ash 0.62%). There are two amorphous structures around 20 2θ. There is a small crystalline peak of calcite. When the XRD spectrum of the fiber powder sample made of PET is examined, the PET in fiber structure is amorphous. Due to its linear structure, there are four amorphous peaks that are wide and have a maximum of around 20 θ (Bian et al., 2022).

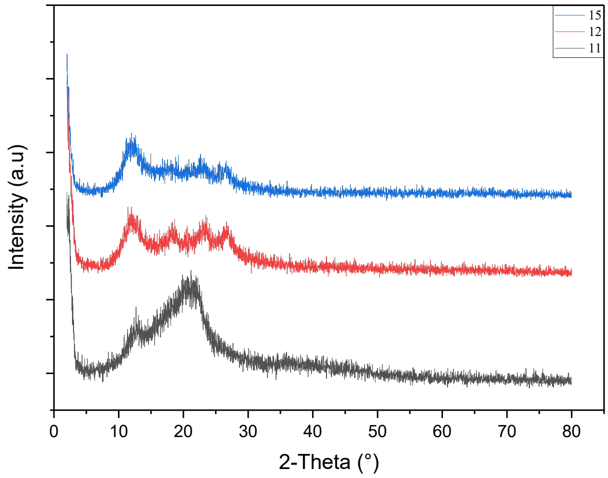

Figure 13. XRD graph of waste polymer in PET structure.

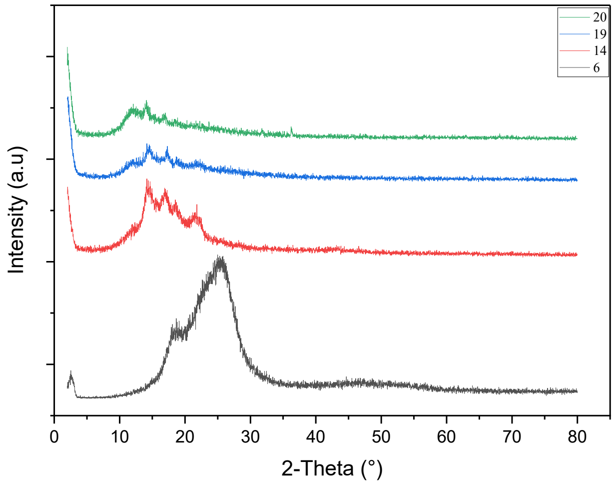

Figure 14. XRD graph of waste polymer in PP structure.

There are 4 different amorphous regions of the flexible flap sample made of PP. In the XRD spectrum of the sack circle sample made of PP, there is a large amorphous structure at 27 2θ (Michell & Müller, 2016).

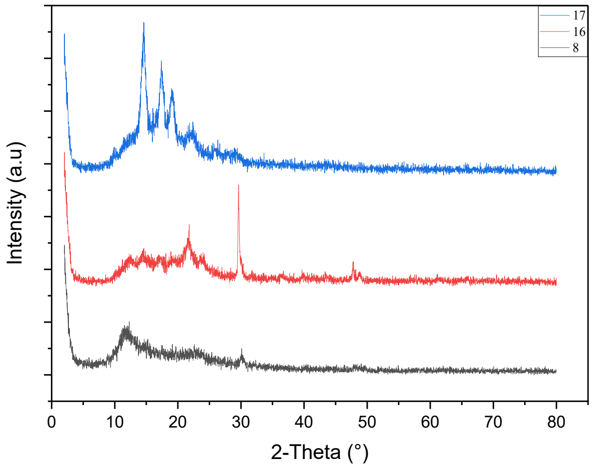

Figure 15. XRD graph of waste polymer in PP structure.

Crystalline peak is seen at 30 2θ of TBS sample (PP+PET+Synthetic Rubber). There is also a calcite peak as an additive in the structure (Sharma et al., 2011).

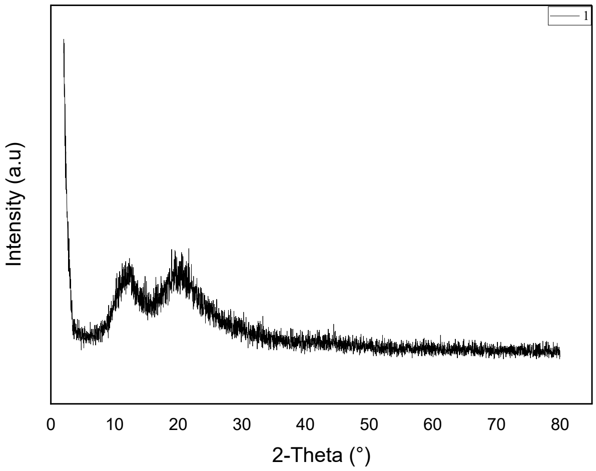

Figure 16. XRD graph of waste polymer in PS structure.

In the XRD spectrum of EPS (expanding polystyrene) foam used in exterior cladding, the structure is largely amorphous. There are two separate amorphous structures in 12 and 22 2θ (Woo et al., 2001).

3.3. SEM analysis results

The results of SEM analysis performed to determine the structural properties of waste polymers and other materials are given below. In Figure 17, the siding foam sample is called expandable (PS, EPS) made of polystyrene. SEM images are in harmony with the literature and have a honeycomb appearance. Since the sample is waste, it is seen that the honeycomb structure is deformed. The thin-walled polystyrene structure between the honeycombs is evident.

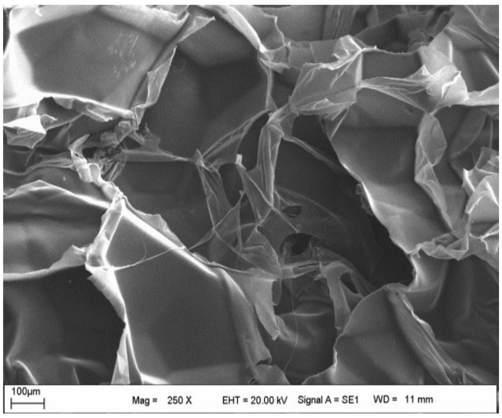

Figure 17. SEM photographs of the exterior coating foam sample (EPS).

SEM image of PE Eco raw material bag contains calcite. The ash value is 16.33%. Calcite particles are clearly visible in the SEM images and the grain size varies. However, it is seen that it is partially homogeneously distributed in PE.

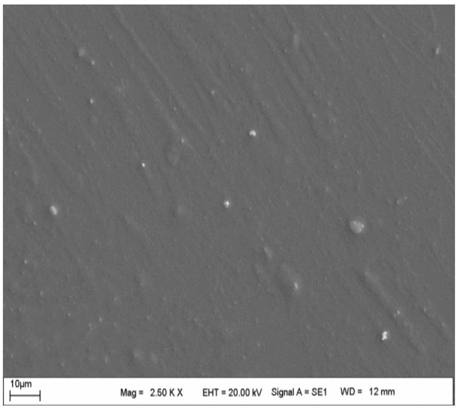

Figure 18. SEM photographs of PE eco raw material bag sample (PE outside aluminum inside).

Figure 19.a. and b. are SEM images of the green and orange cliché band samples, respectively. The only difference between the two samples is the color difference and the material is a PE+PET mixture. SEM images show that both polymers are structurally separated into separate phases. Although it is not a homogeneous mixture, there is a structural harmony. The polymers are adhered to each other.

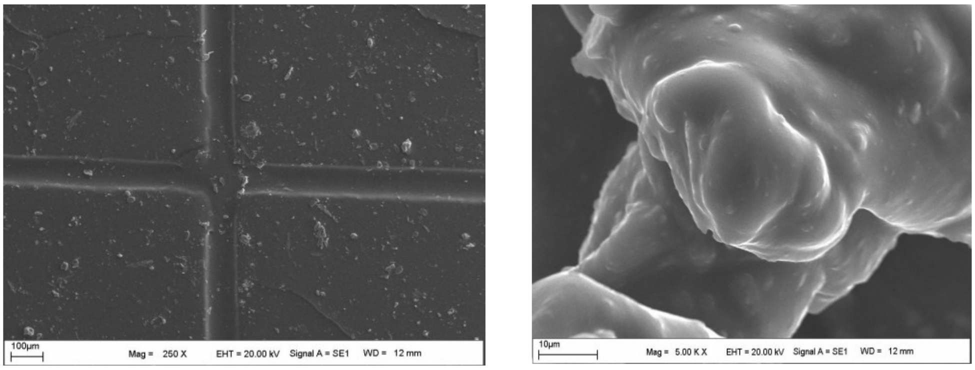

(a) (b)

Figure 19. (a) Green plate tape sample (PE+PET) SEM images, (b) Orange plate tape sample (PE+PET) SEM images.

Figure 20 is the SEM image of the powder sample obtained from PET fiber. PET fibers are clearly visible from the SEM image. The fiber thicknesses are not homogeneous and have different diameters. However, as a result of milling, the fiber structure is not divided into very small pieces. It is seen that there are random breaks at the breaking points of the fiber particles.

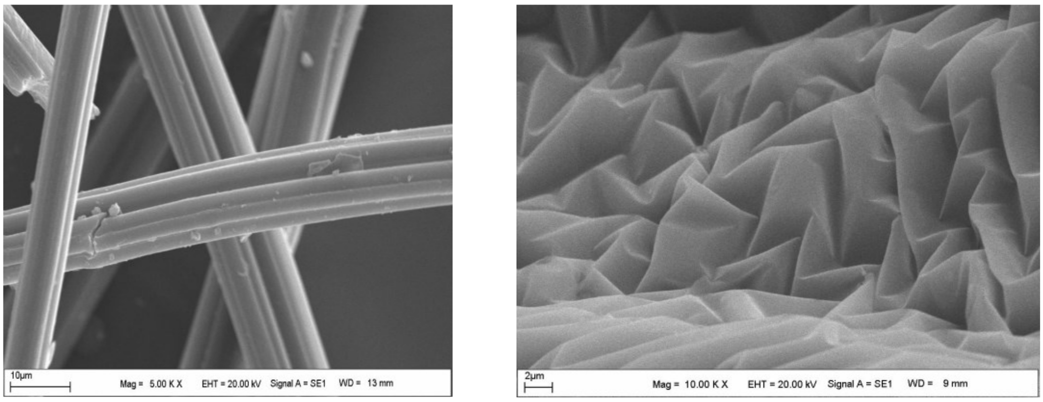

(a) (b)

Figure 20. Fiber powder sample (PET) SEM images.

In Figure 21.a. the PP sack circle sample is shown and it does not contain additives (ash value 0.05%). Structurally, there is a very homogeneous structure present. Contaminations observed on the surface are the ones that have subsequently spread to the structure. In Figure 21.b. SEM image of PET waste spunlace sample is shown. The material has a fiber structure and the diameters of the fibers are very homogeneous, i.e. there is no breakage in the fibers.

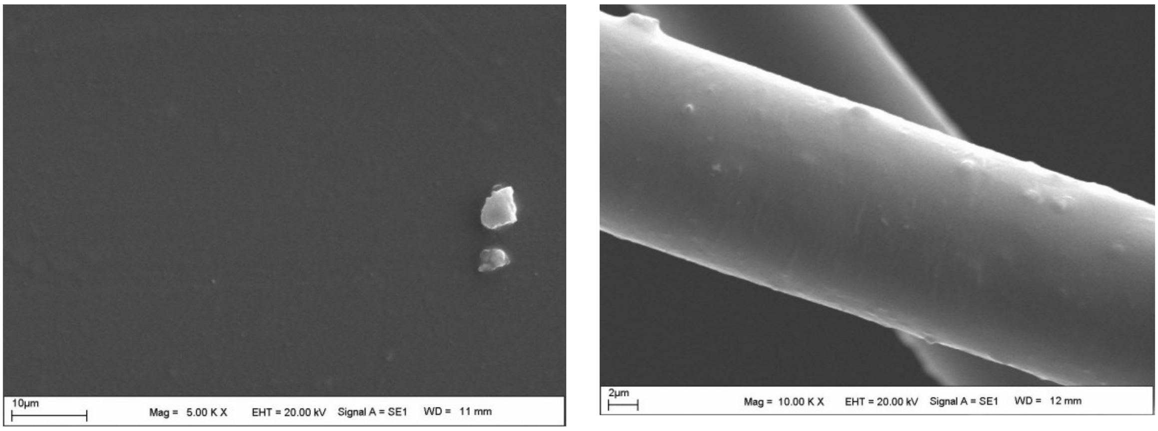

(a) (b)

Figure 21. (a) Sack circle sample (PP) SEM images, (b) Waste spunlace sample (PET) SEM images.

Figure 22.a. It is the SEM image of the packaging in which more polluting substances found in many industries, especially in cement, is shown. The outer part is paper and the inner part is mostly made of PP material. While the paper (cardboard) part has a puffy appearance with a partial air gap, the inner coating of the PP polymer has a thin layered structure. There is no adhesion-like interaction between the paper and the polymer. In Figure 22.b. This is the SEM image of the PET-containing material is shown. It remains solid while recycling the part of the diaper to which the mini side tapes are attached to the front. Ash content is high (15.53%) and appears as a separate phase in the polymer and on the surface. The additive is inorganic and has a calcite structure.

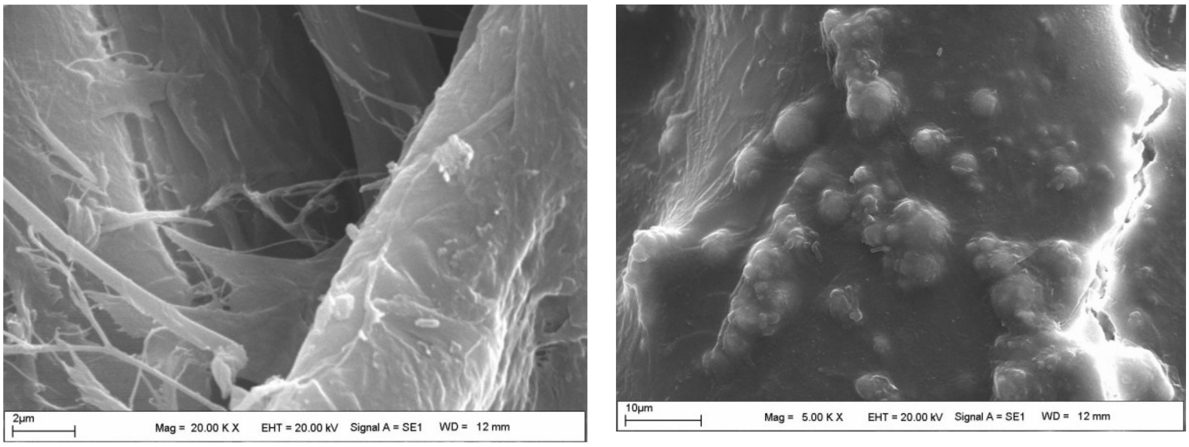

(a) (b)

Figure 22. (a) BZ raw material bag sample (PP+Kraft Paper) SEM images, (b) C band wedge sample (PE+PET+Synthetic Rubber) SEM images.

The SEM image of the polymeric cloth used for cleaning is shown in Figure 23.a. The homogeneous fiber structure is clearly visible and the impurities attached to the fiber are also clearly visible. Inorganic structures resulting from pollutants collected from the environment caused an ash value of 2.54%. As seen from Figure 23.b, SEM image of the cloth used to clean oily impurities and homogeneous polymeric fibers are clearly visible. It is clearly seen that they have structural integrity as a result of the adhesion of the oil to the fiber surface.

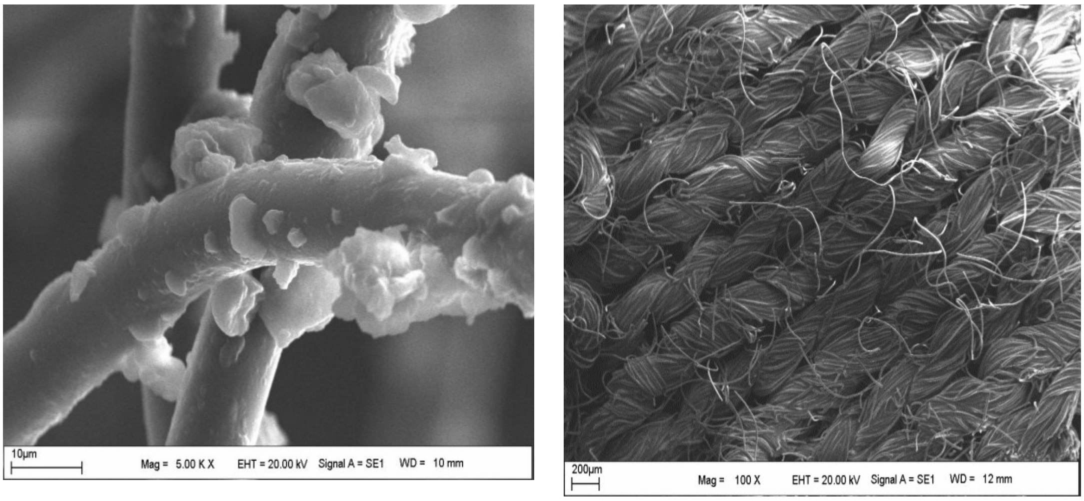

(a) (b)

Figure 23. (a) Dirty cloth sample (PET) SEM images, (b) Oil cloth sample (PET) SEM images.

The sample shown in Figure 24.a is the SEM image of the layer in the diaper that absorbs and diffuses the liquid. The material is in fiber structure and it is seen that the fiber is in the form of a hollow tube. With the help of these channels, the liquid is absorbed and transferred to the other part. The fiber diameter is homogeneous. Figure 24.b. shows the SEM image of the front part of the diaper on which the mini side bands are attached. There is a formation in the form of channels in the fiber structure to ensure adhesion to the surface.

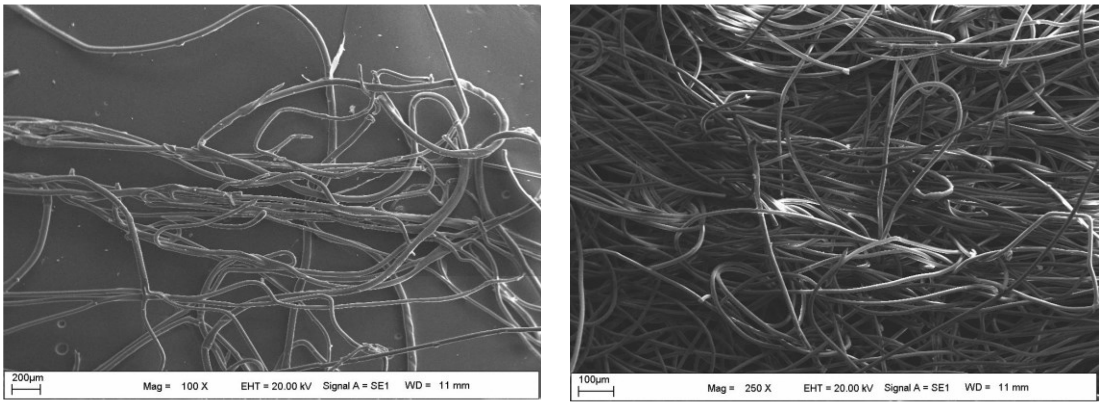

(a) (b)

Figure 24. (a) Green adl sample (PET) SEM images, (b) C band sample (PE+PET+Synthetic Rubber) SEM images.

There are flexible parts on the sides of the diaper and it is a material made of PP (Figure 25.a). It is produced in the form of filaments of different diameters to increase flexibility throughout the material and prevent breakage. Figure 25.b. shows the part that absorbs and spreads the liquid in the baby diaper made of PET and consists of fibers that have been converted into cotton. Since PET fiber surfaces are thinned too much, water is retained by hydrogen bonding at the carbonyl groups and polymer end ends on the surface and the liquid is absorbed.

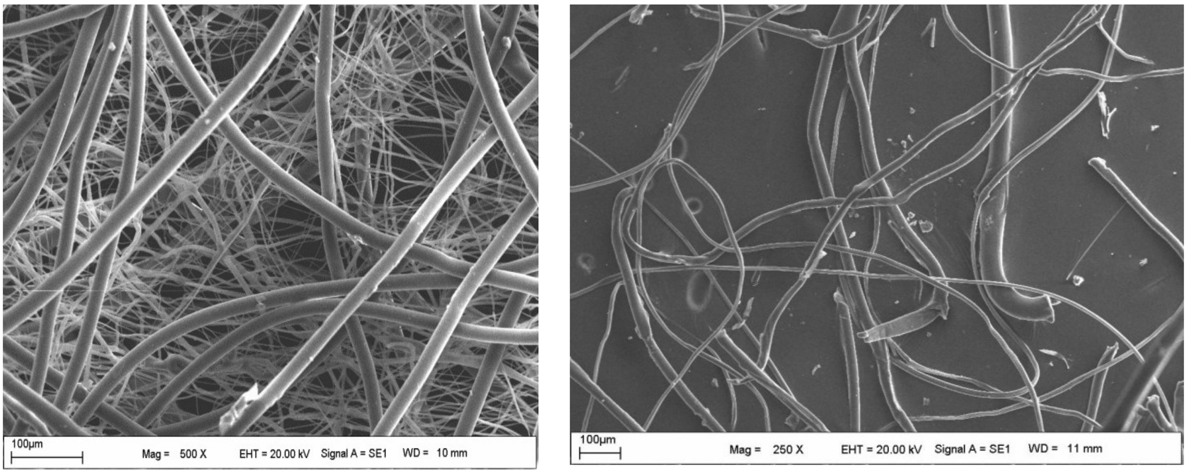

(a) (b)

Figure 25. (a) Flexible atria sample (PP) SEM images, (b) White adl sample (PET) SEM images.

Figure 26.a. the diaper made of PE-PP contains the SEM image of the outermost layer. PE and PP have been transformed into a very thin filament form to increase flexibility and to allow the skin to breathe. Figure 26.b. SEM image of mini sideband sample made of PP. The material is a very flexible material and is in filament form. The SEM image shows that the fibers are homogeneous and intertwined. This structure contributes to its flexibility.

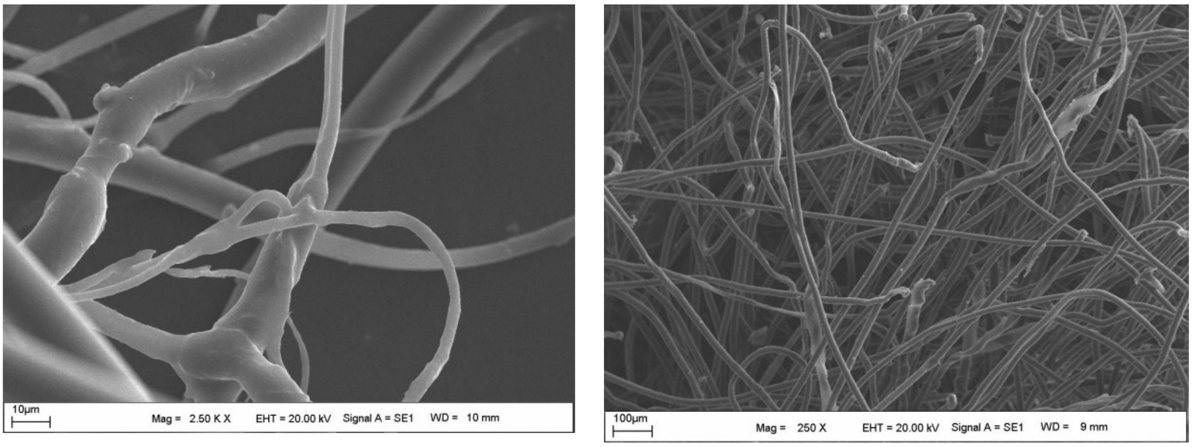

(a) (b)

Figure 26. (a) TBS sample (PE+PP+Synthetic Rubber) SEM images, (b) Mini sideband sample (PP+Synthetic Rubber) SEM images.

Figure 27.a. SEM image of outermost layer of diaper made of PE and PET. From the SEM images, it is seen that both polymers are in fiber structure. While PE provides flexibility to the material, PET creates a barrier to prevent the liquid inside from escaping. It is clearly seen that the fibers are of very homogeneous diameter. Figure 27.b. It is the SEM image of the part that prevents the liquid from coming out on the side parts made of PP. Thin fibers were formed in order to provide impermeability by interpenetrating each other in different diameters by stripping the PP surfaces. Since PP does not hydrogen bond with water, this structure provides an extra contribution.

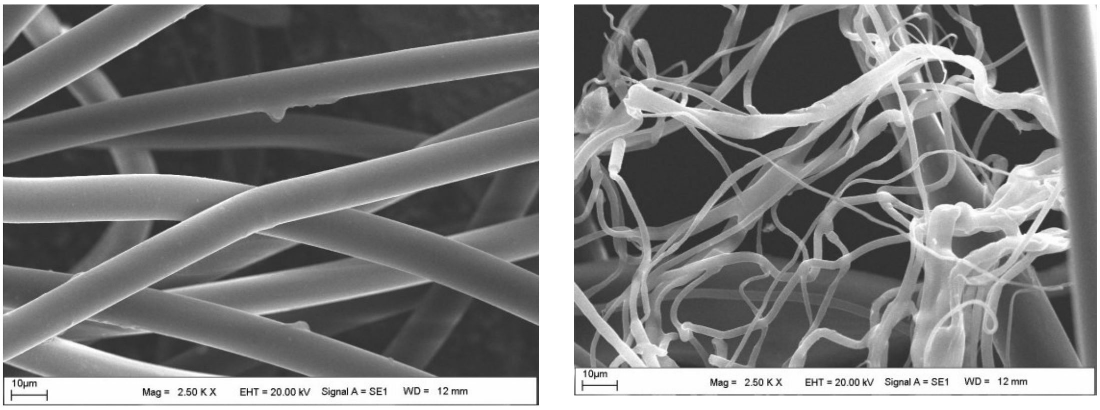

(a) (b)

Figure 27. (a) SBS sample (PE+PET+Synthetic Rubber) SEM images, (b) Barrier sample (PP) SEM images.

Figure 28 it contains the SEM image of the part that receives the liquid made of PP and transmits it to a substrate. Although the SEM image is similar to the previous structure, this structure has the appearance of a partially sieve structure. Since PP does not like water, the sieve structure is designed to allow the liquid to pass down to the part that holds the liquid.

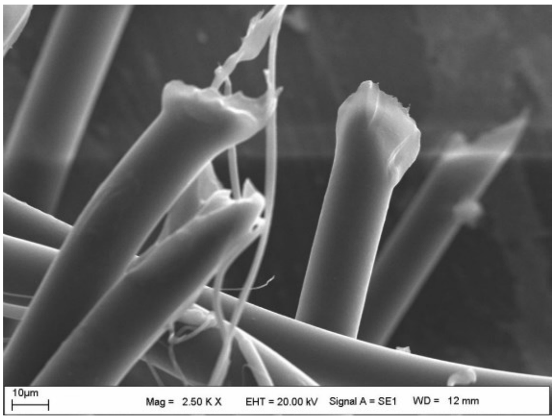

Figure 28. Tissue sample (PP) SEM images.

3.4. TGA-DTA analysis results

Figures 29-37 are DSC-TG spectra of some of the samples studied, respectively. Figure 29 is a green ADL (PET) material with exothermic peak maximums at 245, 360, 450 and 560°C. The ash value was low (0.07%) and the TG value was close to zero. Depending on the ethylene and terephthalic acid groups in the PET structure and the chain structure of the polymer, exothermic decomposition peaks at different temperatures are the expected result (Ng et al., 2002).

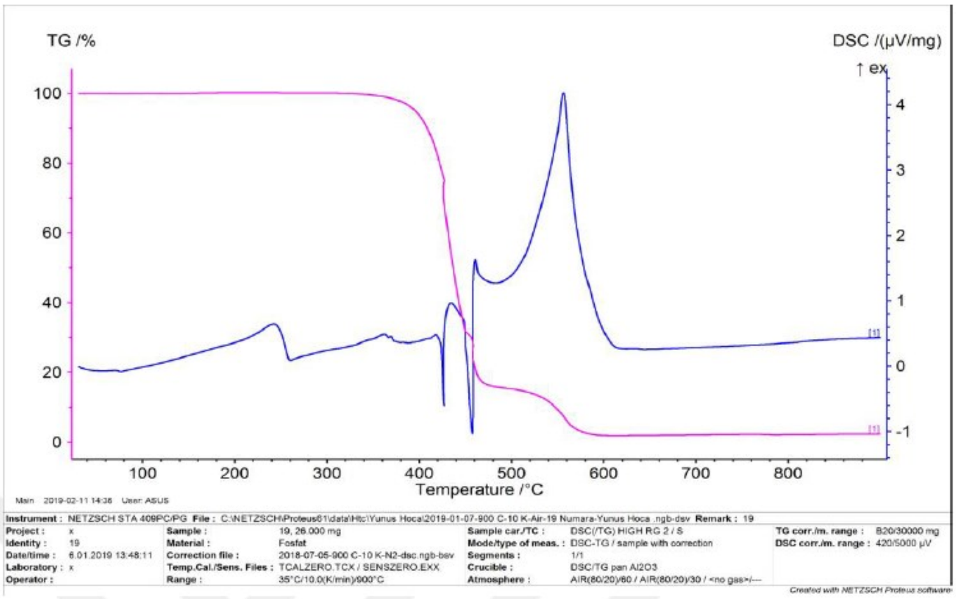

Instrument : NETZSCH STA 409PC/PG File : C:\NETZSCH\Proteus61\data\Htc\Yunus Hoca\2019-01-07-900 C-10 K-Air-19 Numara-Yunus Hoca .ngb-dsv Remark : 19
Project : x
Identity : 19
Date/time : 6.01.2019 13:48:11
Laboratory : x
Operator :
Sample : 19, 26.000 mg
Material : Fosfat
Correction file : 2018-07-05-900 C-10 K-N2-dsc.ngb-bsv
Temp.Cal./Sens. Files : TCALZERO.TCX / SENSZERO.EXX
Range : 35°C/10.0(K/min)/900°C
Sample car./TC : DSC(/TG) HIGH RG 2 / S
Mode/type of meas. : DSC-TG / sample with correction
Segments : 1/1
Crucible : DSC/TG pan Al2O3
Atmosphere : AIR(80/20)/60 / AIR(80/20)/30 / <no gas>/---
TG corr./m. range : 820/30000 mg
DSC corr./m. range : 420/5000 µV

Figure 29. Green ADL sample (12) (PET) thermal analysis chart.

Figure 30 is the DSC-TG thermal decomposition spectrum of the PE+PET+Synthetic Rubber mixture material, and the endothermic peak at 125°C indicates the removal of water, and the exothermic peaks at 240, 420, 440, 480 and 540°C belong to the thermal decomposition of all three polymers. The ash value of the material is 0.25% and the TG value is close to zero (Prime et al., 2009).

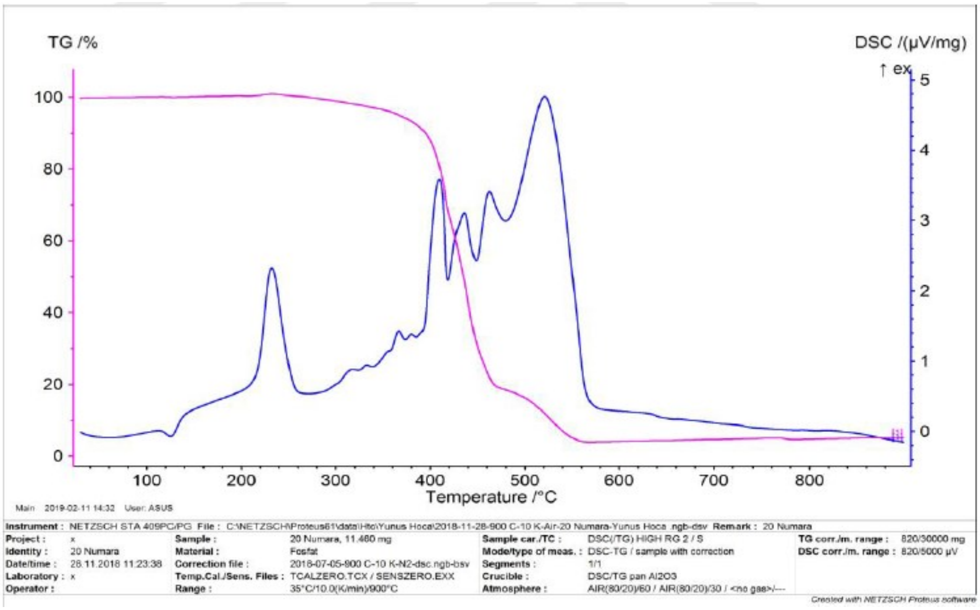

Instrument : NETZSCH STA 409PC/PG File : C:\NETZSCH\Proteus61\data\Htc\Yunus Hoca\2018-11-28-900 C-10 K-Air-20 Numara-Yunus Hoca .ngb-dsv Remark : 20 Numara
Project : x
Identity : 20 Numara
Date/time : 28.11.2018 11:23:38
Laboratory : x
Operator :
Sample : 20 Numara, 11.460 mg
Material : Fosfat
Correction file : 2018-07-05-900 C-10 K-N2-dsc.ngb-bsv
Temp.Cal./Sens. Files : TCALZERO.TCX / SENSZERO.EXX
Range : 35°C/10.0(K/min)/900°C
Sample car./TC : DSC(/TG) HIGH RG 2 / S
Mode/type of meas. : DSC-TG / sample with correction
Segments : 1/1
Crucible : DSC/TG pan Al2O3
Atmosphere : AIR(80/20)/60 / AIR(80/20)/30 / <no gas>/---
TG corr./m. range : 820/30000 mg
DSC corr./m. range : 820/5000 µV

Figure 30. C-Tape sample (13) (PE+PET+Synthetic Rubber) thermal analysis chart.

Figure 31 is the DSC-TG spectrum of the flexible tab material made of PP. The endothermic peak at 160°C belongs to the melting of PP, and the 360, 400 and 460°C exothermic peaks are the thermal degradation peaks of PP (Doyle, 1961). The ash value is zero and the TG value is close to zero.

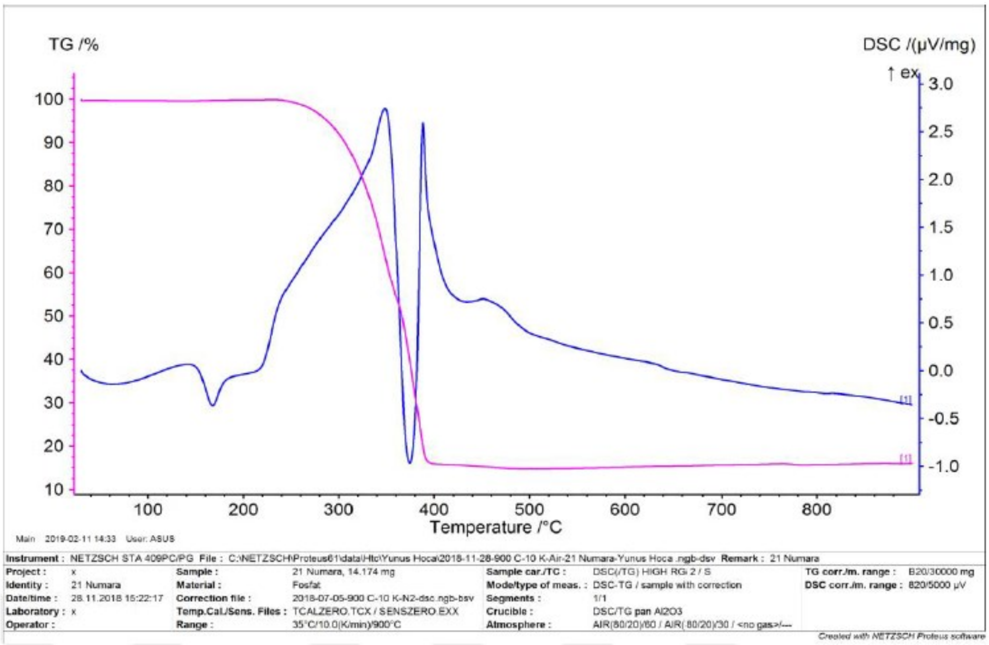

Main 2019-02-11 14:33 User: ASUS

Instrument : NETZSCH STA 409PC/PG File : C:\NETZSCH\Proteus61\data\Htc\Yunus Hoca\2018-11-28-900 C-10 K-Air-21 Numara-Yunus Hoca .ngb-dsv Remark : 21 Numara
Project : x
Identity : 21 Numara
Date/time : 28.11.2018 15:22:17
Laboratory : x
Operator :
Sample : 21 Numara, 14.174 mg
Material : Fosfat
Correction file : 2018-07-05-900 C-10 K-N2-dsc.ngb-bsv
Temp.Cal./Sens. Files : TCALZERO.TCX / SENSZERO.EXX
Range : 35°C/10.0(K/min)/900°C
Sample car./TC : DSC(/TG) HIGH RG 2 / S
Mode/type of meas. : DSC-TG / sample with correction
Segments : 1/1
Crucible : DSC/TG pan Al2O3
Atmosphere : AIR(80/20)/60 / AIR(80/20)/30 / <no gas>/---
TG corr./m. range : B20/30000 mg
DSC corr./m. range : 820/5000 µV

Figure 31. Flexible ear sample (14) (PP) thermal analysis chart.

Figure 32 is the DSC-TG spectrum of the white ADL material made of PET. An endothermic peak is observed at 260°C and an exothermic peak at 440 and 520°C.

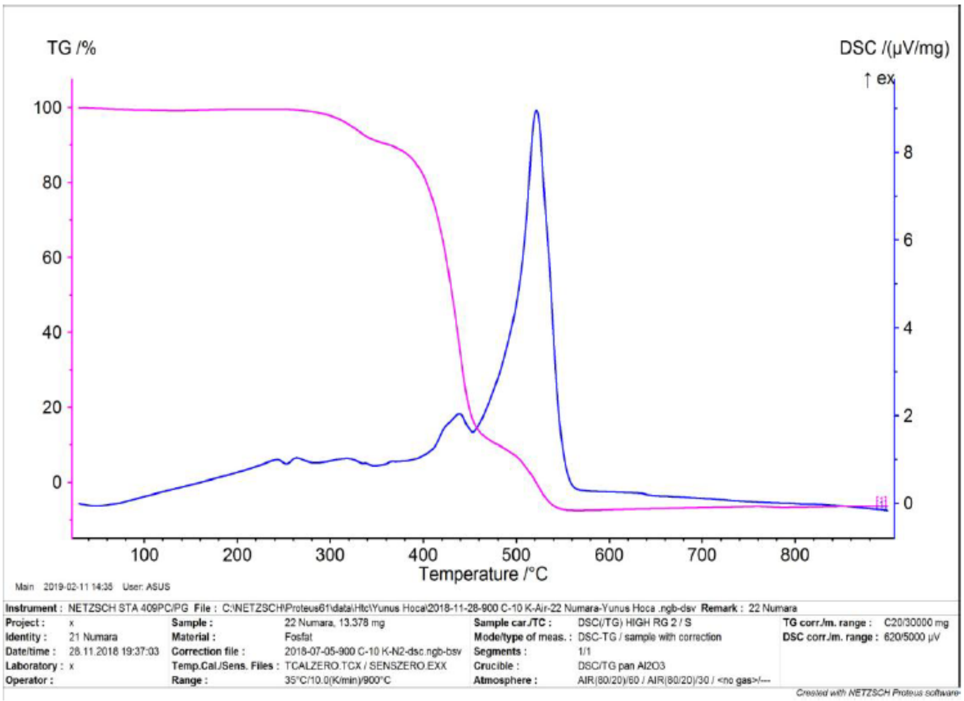

Main 2019-02-11 14:35 User: ASUS

Instrument : NETZSCH STA 409PC/PG File : C:\NETZSCH\Proteus61\data\Htc\Yunus Hoca\2018-11-28-900 C-10 K-Air-22 Numara-Yunus Hoca .ngb-dsv Remark : 22 Numara
Project : x
Identity : 21 Numara
Date/time : 28.11.2018 19:37:03
Laboratory : x
Operator :
Sample : 22 Numara, 13.378 mg
Material : Fosfat
Correction file : 2018-07-05-900 C-10 K-N2-dsc.ngb-bsv
Temp.Cal./Sens. Files : TCALZERO.TCX / SENSZERO.EXX
Range : 35°C/10.0(K/min)/900°C
Sample car./TC : DSC(/TG) HIGH RG 2 / S
Mode/type of meas. : DSC-TG / sample with correction
Segments : 1/1
Crucible : DSC/TG pan Al2O3
Atmosphere : AIR(80/20)/60 / AIR(80/20)/30 / <no gas>/---
TG corr./m. range : C20/30000 mg
DSC corr./m. range : 620/5000 µV

Figure 32. White ADL sample (15) (PET) thermal analysis chart.

Figure 33 DSC-TG thermal degradation spectrum of PP+PE+ Synthetic Rubber mixture material is given. Two endothermic peaks at temperatures of 170 and 240°C belong to the melting of polymeric materials. The exothermic peaks at 380 and 480°C are the degradation peaks of the polymer mixture. In addition, an endothermic peak of around 700°C is observed for the inorganic additive.

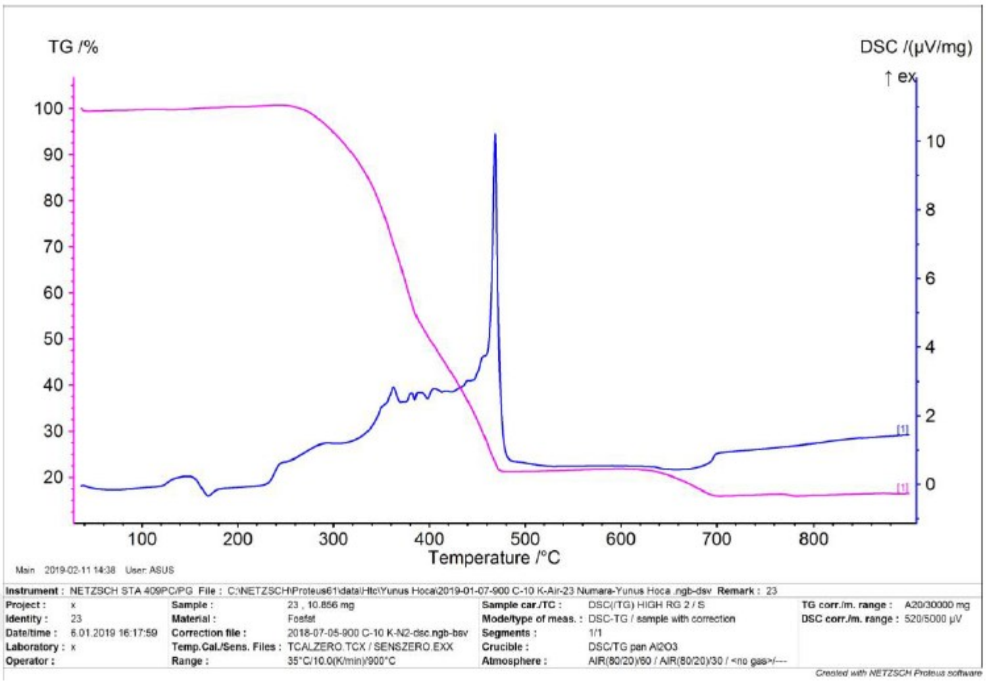

Figure 33. TBS sample (16) (PP+PE+ Synthetic Rubber) thermal analysis chart.

Figure 34 is the DSC-TG thermal degradation spectrum of the mini sideband material made of PP+Synthetic Rubber. The endothermic peak of the melting of PP at 180°C and the broadband exothermic peak with the peak maximum at 400°C belong to the thermal decomposition of PP.

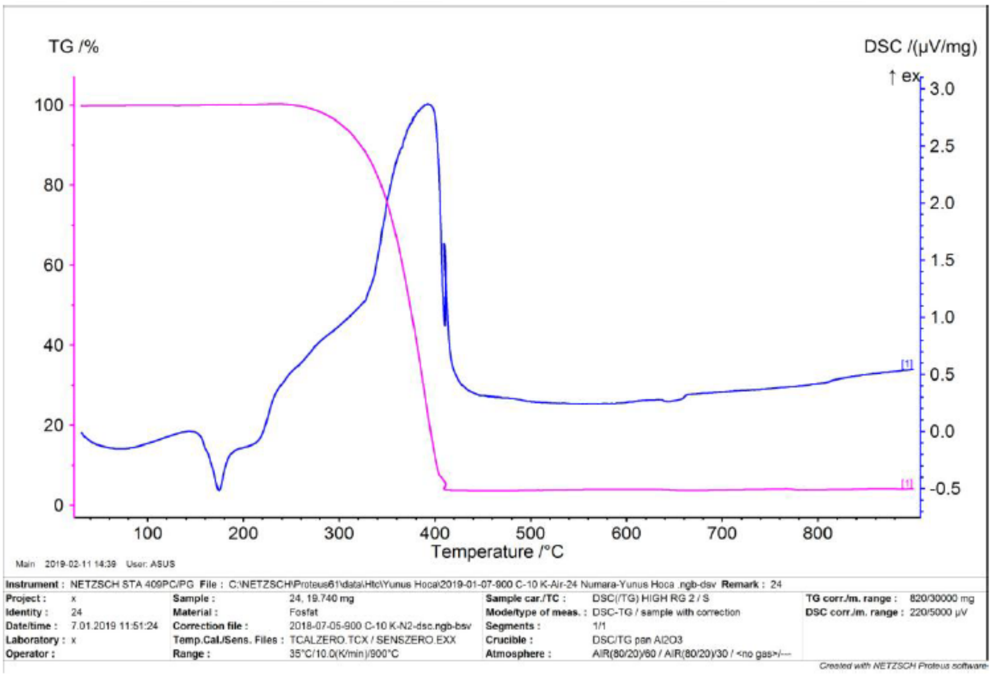

Figure 34. Mini sideband sample (17) (PP+Synthetic Rubber) thermal analysis chart.

Figure 35 is the DSC-TG thermal degradation spectrum of PE+PET+Synthetic Rubber mixture SBS material. The endothermic peak in the form of a broad band in the temperature range of 260-360°C belongs to the melting of the polymer mixture. Exothermic peaks at 400, 460 and 520°C are the degradation peaks of the polymeric mixture. The endothermic decomposition peak of the inorganic additive is clearly visible at 740°C (Doyle, 1961).

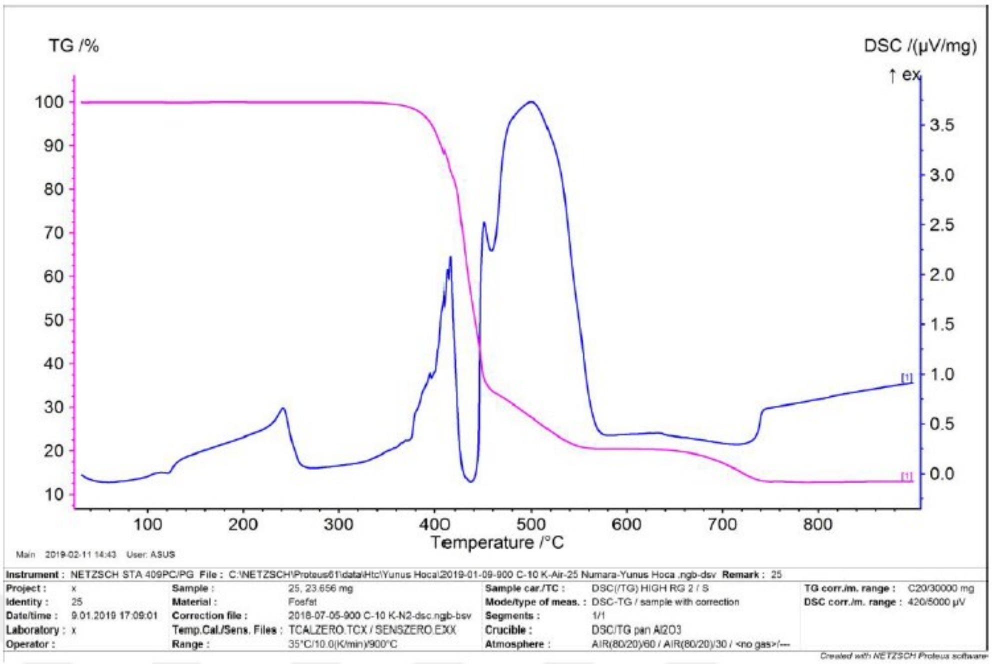

Instrument : NETZSCH STA 409PC/PG File : C:\NETZSCH\Proteus61\data\Htc\Yunus Hoca\2019-01-09-900 C-10 K-Air-25 Numara-Yunus Hoca .ngb-dsv Remark : 25
Project : x
Identity : 25
Date/time : 9.01.2019 17:09:01
Laboratory : x
Operator :
Sample : 25, 23.656 mg
Material : Fosfat
Correction file : 2018-07-05-900 C-10 K-N2-dsc.ngb-bsv
Temp.Cal./Sens. Files : TCALZERO.TCX / SENSZERO.EXX
Range : 35°C/10.0(K/min)/900°C
Sample car./TC : DSC(/TG) HIGH RG 2 / S
Mode/type of meas. : DSC-TG / sample with correction
Segments : 1/1
Crucible : DSC/TG pan Al2O3
Atmosphere : AIR(80/20)/60 / AIR(80/20)/30 / <no gas>/---
TG corr./m. range : C20/30000 mg
DSC corr./m. range : 420/5000 µV

Figure 35. SBS sample (18) (PE+PET+ Synthetic Rubber) thermal analysis chart.

Figures 36 and 37 are DSC-TG thermal degradation spectra of barrier and tissue materials made of PP. The endothermic peak of both samples at 170°C belongs to the melting of PP, and the exothermic peak at 390°C belongs to the thermal degradation of PP (Yuan et al., 2021).

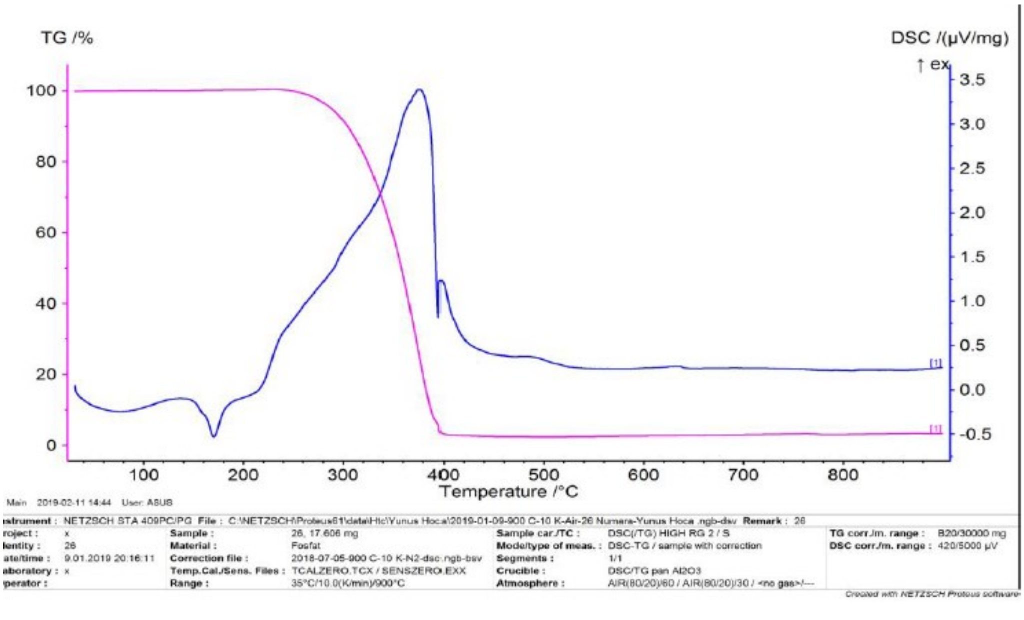

strument : NETZSCH STA 409PC/PG File : C:\NETZSCH\Proteus61\data\Htc\Yunus Hoca\2019-01-09-900 C-10 K-Air-26 Numara-Yunus Hoca .ngb-dsv Remark : 26
roject : x
lentity : 26
ate/time : 9.01.2019 20:16:11
aboratory : x
perator :
Sample : 26, 17.606 mg
Material : Fosfat
Correction file : 2018-07-05-900 C-10 K-N2-dsc.ngb-bsv
Temp.Cal./Sens. Files : TCALZERO.TCX / SENSZERO.EXX
Range : 35°C/10.0(K/min)/900°C
Sample car./TC : DSC(/TG) HIGH RG 2 / S
Mode/type of meas. : DSC-TG / sample with correction
Segments : 1/1
Crucible : DSC/TG pan Al2O3
Atmosphere : AIR(80/20)/60 / AIR(80/20)/30 / <no gas>/---
TG corr./m. range : B20/30000 mg
DSC corr./m. range : 420/5000 µV

Figure 36. Barrier sample (19) (PP) thermal analysis chart.

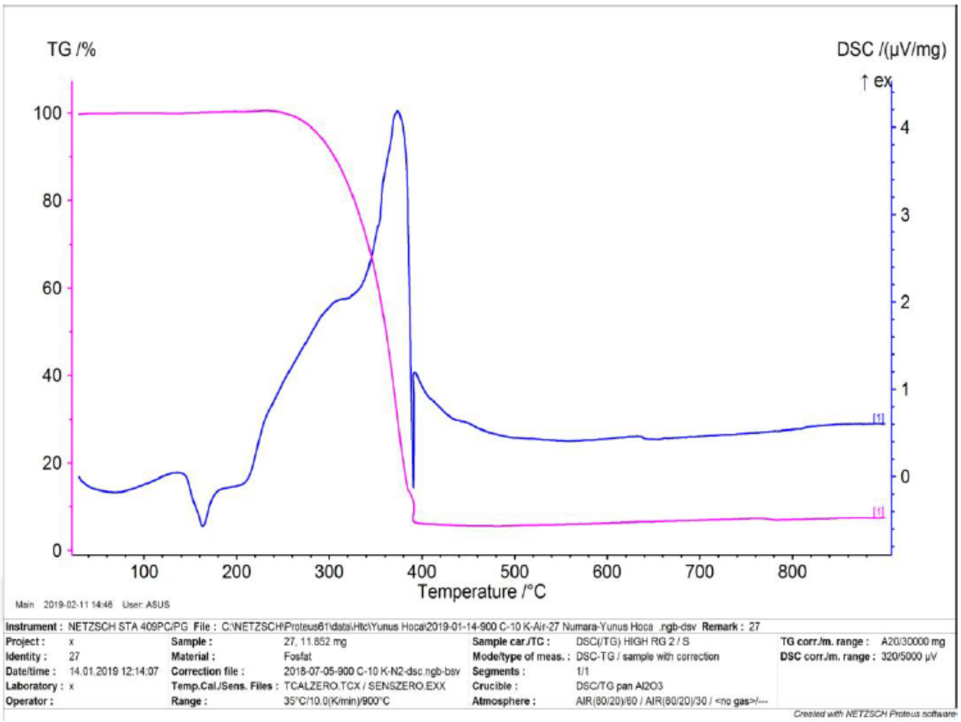

Instrument : NETZSCH STA 409PC/PG File : C:\NETZSCH\Proteus61\data\Htc\Yunus Hoca\2019-01-14-900 C-10 K-Air-27 Numara-Yunus Hoca .ngb-dsv Remark : 27
Project : x
Identity : 27
Date/time : 14.01.2019 12:14:07
Laboratory : x
Operator :
Sample : 27, 11.852 mg
Material : Fosfat
Correction file : 2018-07-05-900 C-10 K-N2-dsc.ngb-bsv
Temp.Cal./Sens. Files : TCALZERO.TCX / SENSZERO.EXX
Range : 35°C/10.0(K/min)/900°C
Sample car./TC : DSC(/TG) HIGH RG 2 / S
Mode/type of meas. : DSC-TG / sample with correction
Segments : 1/1
Crucible : DSC/TG pan Al2O3
Atmosphere : AIR(80/20)/60 / AIR(80/20)/30 / <no gas>/---
TG corr./m. range : A20/30000 mg
DSC corr./m. range : 320/5000 µV

Figure 37. Tissue sample (20) (PP) thermal analysis chart.

3.5. Calorific value analysis results

The LHV and HHV values obtained as a result of the thermal value analysis are given in Table 7.

Table 7. Calorific value of polymeric waste

Sample	**Lower heating value (LHV) (cal/g)**	**Higher heating value (HHV) (cal/g)**	**Sample**	**Lower heating value (LHV) (cal/g)**	**Higher heating value (HHV) (cal/g)**
Exterior Cladding (Foam)	9 444	9 065	Oily Cloth	7 134	6 713
Eco Raw Material Bag (Outside Aluminum)	9 902	9 422	Green Adl Sample	4 655	4 462
Green Cliche Tape	8 836	8 317	C Band Sample	6 646	6 316
Orange Cliche Tape	8 451	7 973	Flexible Ear Sample	10 797	10 103
Fiber Powder	4 491	4 292	White Adl Sample	5 007	4 783
Sack Circle	5 543	5 334	Tbs Sample	8 921	8 344
Waste Spunlace Fabric	5 548	5 289	Mini Sideband Sample	10 578	9 941
Bz Raw Material Bag	6 585	6 156	Sbs Sample	5 396	5 207
C Band Wedge	7 008	6 648	Barrier Sample	10 965	10 305
Dirty Cloth	6 220	6 017	Tissue Sample	10 525	9 844

Calorific values of all samples are in the range of 4 292-10 965 cal/g values. When wastes are evaluated in terms of energy production, the amount of waste is very high. For this reason, waste recycling is at a level that can be achieved with incineration systems. When the thermal values are examined, enough energy can be obtained from wastes to meet all the energy needs of the enterprise. In this study, thermal values of waste polymers are given. The total amount of energy is 18 790 MJ/hour (Akdağ, 2019) (This value has been calculated by evaluating all the wastes produced in the factory.)

4. Discussion and Conclusion

The waste amounts for 2017, 2018 and 2019 at the factory are given in the table below by the month.

Table 8. The waste amounts for 2017, 2018, and 2019 years

2017		**2018**		**2019**	
Months	**Waste amount (kg)**	**Months**	**Waste amount (kg)**	**Months**	**Waste amount (kg)**
July	543 197	January	443 712	January	263 808
August	513 030	February	431 254	February	256 135
September	356 980	March	411 220	March	330 221
October	311 940	April	397 680	April	339 476
November	319 966	May	353 454	May	304 328
December	419 840	June	350 730	June	203 562
		July	400 760	July	319 194
		August	429 106	August	237 217
		September	268 168		
		October	357 317		
		November	260 255		
		December	270 166		

As can be seen from the table, the amount of waste is increasing every year. For this reason, the measured calorie values of the wastes, FT-IR, XRD, SEM, TGA-DTA graphics gave information about the pollution status of the wastes. As a result of the thermal value analysis, a total energy value of 18 790 MJ/hour emerges. When the Bz raw material bag materials in stock in the factory are burned regularly within 3 years, an energy value of 108 MJ/hour is obtained, and when the calculation is made for C band waste materials, an energy value of 1 586 MJ/hour. In total, 18 790 + 108 + 1 586 = 20 484 MJ/hour energy can be obtained. This energy can be used to generate electricity. If it is used in electricity generation, 2,276 MWh of electricity production emerges. The production capacity of the factory continues to increase. It is thought that the amount of energy will remain constant even if the wastes in the stock are finished. Waste polymers from this factory are not suitable to be disposed of in the landfill. Waste should be stocked. And it should be used in electricity generation by direct combustion. In this way, it should be brought back to the economy. According to the characterization results, the basic compositions of the wastes did not change. The structure has been preserved. Polyethylene, polypropylene, polystyrene, and polyethylene terephthalate polymers in the structure of the sanitary napkins, diapers, patient diapers and by-products studied did not undergo any chemical change. In this case, these raw materials can be reused in different areas of the industry.

Studies in the literature evaluating polymer wastes are given in Table 9. Existing factory waste products can be used as a source of raw materials in the fields of textile, insulation, toys, automotive, health, bottles, as in these studies. When their structural properties are examined, it has been determined that polymer types are widely used in industry (Tayyar & Üstün, 2010; Çınar & Kar, 2018; Padhan & Gupta, 2018; Dieterich et al., 2020).

Table 9. Previous studies on the evaluation of polymeric wastes

Reclaimed polymer	**Usage Areas**	**Reference**
Polyethylene (PE)	Industrial uses and road applications, composite production, production of jerrycans, bottles, plates and toys	(Achilias et al., 2008; Duarte & Faxina, 2021)
Polypropylene (PP)	Insulation applications, yoghurt cups, suitcases, pipes, buckets	(Tayyar & Üstün, 2010; Tufan et al., 2015)
Polyethylene Terephthalate (PET)	It is used to make food and Beverage bottles and synthetic yarn., fiber and so on.	(Ahrabi et al., 2012; El-Saftawy et al., 2014; Sharma et al., 2011)
Polystyrene (PS)	Yogurt cups, foam packs, cassettes, thermal insulation material	(Demirkır et al., 2017; Özsin & Pütün, 2018; Woo et al., 2001)
Polyethylene (PE), Polyethylene Terephthalate (PET), acrylonitrile butadiene styrene	Bags, sacks, and wraps, other packaging, other containers, and soft drink, milk, and water containers, appliances, furniture, casings of lead-acid batteries, and other products.	(Al-Salem et al., 2009)
Polyethylene (PE), Polypropylene (PP)	Packaging film, bags, pipes	(Achilias et al., 2007)
Polyethylene terephthalate (PET)	Packaging, food, beverage and automotive industries	(Ghosal & Nayak, 2022; Raheem et al., 2019)

It is possible to obtain heat energy by incineration of wastes directly. Polymeric wastes can be used for energy recovery in the industry, and thus energy costs can be reduced. The results of the thermal analysis and calorific values of wastes showed that a significant part of the electricity need of the factory could be met. The recovery heat energy can be used to convert water to steam in steam boilers, to run electric generators, and to generate heating and hot water. In this way, energy savings will be achieved, and environmental pollution will be reduced by waste disposal by incineration.

Acknowledgements

We would like to thank Inonu University Scientific Research Projects Unit for their support within the scope of the project numbered FYL-2018 1462. Author Yeliz Toptaş, within the scope of YÖK 100/2000 PhD Project, by the Council of Higher Education in the sub-field of Fuels (Fossil and Bio) and Combustion; It is supported by TUBITAK with 2211-C Domestic Priority Fields Doctoral Scholarship Program.

References

Achilias, D. S., Roupakias, C., Megalokonomos, P., Lappas, A. A., & Antonakou, E. V. (2007). Chemical recycling of plastic wastes made from polyethylene (LDPE and HDPE) and polypropylene (PP). *Journal of Hazardous Materials*, 149(3), 536 - 542. doi:10.1016/j.jhazmat.2007.06.076

Achilias, D. S., Antonakou, E., Roupakias, C., Megalokonomos, P., & Lappas, A. (2008). Recycling techniques of polyolefins from plastic wastes. *Global NEST Journal*, 10(1), 114 - 122.

Ahrabi, A. Z., Bilici, I., & Bilgesü, A. Y. (2012). Pet atiklari kullanilarak kompozit malzeme üretiminin araştirilmasi. *Journal of the Faculty of Engineering and Architecture of Gazi University*, 27(3), 467 - 471.

Akdağ, H. (2019). *Eruslu global grup firmalarındaki atık polimerlerin karakterizasyonu ve piroliz-yakma yöntemleri kullanılarak enerji üretimi fizibilitesinin hazırlanması*. (M.Sc.) İnönü Üniversitesi, Fen Bilimleri Enstitüsü, Türkiye.

Al-Salem, S. M., Lettieri, P., & Baeyens, J. (2009). Recycling and recovery routes of plastic solid waste (PSW): A review. *Waste Management*, 29(10), 2625 - 2643.

doi:10.1016/j.wasman.2009.06.004

Arutchelvi, J., Sudhakar, M., Arkatkar, A., Doble, M., Bhaduri, S., & Uppara, P. V. (2008). Biodegradation of polyethylene and polypropylene. *Indian Journal of Biotechnol*ogy, 7(1), 9-22.

Asgari, P., Moradi, O., & Tajeddin, B. (2014). The effect of nanocomposite packaging carbon nanotube base on organoleptic and fungal growth of Mazafati brand dates. *International Nano Letters*, 4, 1 - 5. doi:10.1007/s40089-014-0098-3

Baechler, C., DeVuono, M., & Pearce, J. M. (2013). Distributed recycling of waste polymer into RepRap feedstock. *Rapid Prototyping Journal*, 19(2), 118 - 125. doi:10.1108/13552541311302978

Bahoria, B. V, Parbat, D. K., & Nagarnaik, P. B. (2018). XRD analysis of natural sand, quarry dust, waste plastic (ldpe) to be used as a fine aggregate in concrete. *Materials Today: Proceedings*, 5(1), 1432 - 1438. doi:10.1016/j.matpr.2017.11.230

Barrios, V. A. E., Méndez, J. R. R., Aguilar, N. V. P., Espinosa, G. A., & Rodríguez, J. L. D. (2012). FTIR-An Essential Characterization Technique for Polymeric Materials. In T. Theophanides (Ed.), *Infrared Spectroscopy - Materials Science, Engineering and Technology* (pp. 195-212). InTech. doi:10.5772/36044

Bian, L., Dong, Y., & Jiang, B. (2022). Simplified creation of polyester fabric supported Fe-based MOFs by an industrialized dyeing process: Conditions optimization, photocatalytics activity and polyvinyl alcohol removal. *Journal of Environmental Sciences*, 116, 52 - 67. doi:10.1016/j.jes.2021.06.007

Campbell, D., Pethrick, R. A., & White, J. R. (2000). *Polymer Characterization: Physical Techniques*. London, UK: CRC press.

Caro, E., & Comas, E. (2017). Polyethylene comonomer characterization by using FTIR and a multivariate classification technique. *Talanta*, 163, 48 - 53. doi:0.1016/j.talanta.2016.10.082

Chalmers, J. M., & Everall, N. J. (1999). Polymer analysis and characterization by FTIR, FTIR-microscopy, Raman spectroscopy and chemometrics. *International Journal of Polymer Analysis and Characterization*, 5(3), 223 - 245. doi:10.1080/10236669908009739

Çınar, M. E., & Kar, F. (2018). Characterization of composite produced from waste PET and marble dust. *Construction and Building Materials*, 163, 734 - 741. doi:10.1016/j.conbuildmat.2017.12.155

Costa, L. M. B., Silva, H. M. R. D., Peralta, J., & Oliveira, J. R. M. (2019). Using waste polymers as a reliable alternative for asphalt binder modification–Performance and morphological assessment. *Construction and Building Materials*, 198, 237 - 244. doi:10.1016/j.conbuildmat.2018.11.279

da Silva, D. J., & Wiebeck, H. (2020). Current options for characterizing, sorting, and recycling polymeric waste. *Progress in Rubber, Plastics and Recycling Technology*, 36(4), 284 - 303. doi:10.1177/1477760620918603

Demirkır, C., Öztürk, H., & Çolakoğlu, G. (2017). Effects of press parameters on some technological properties of polystren composite plywood. *Kastamonu University Journal of Forestry Faculty*, 17(3), 517 - 522. doi: 10.17475/kastorman.285645

Dieterich, V., Buttler, A., Hanel, A., Spliethoff, H., & Fendt, S. (2020). Power-to-liquid via synthesis of methanol, DME or Fischer–Tropsch-fuels: a review. *Energy & Environmental Science*, 13(10), 3207 - 3252. doi:10.1039/D0EE01187H

Doyle, C. D. (1961). Estimating thermal stability of experimental polymers by empirical thermogravimetric analysis. *Analytical Chemistry*, 33(1), 77 - 79. doi:10.1021/ac60169a022

Duarte, G. M., & Faxina, A. L. (2021). Asphalt concrete mixtures modified with polymeric waste by the wet and dry processes: A literature review. *Construction and Building Materials*, 312, 125408. doi:10.1016/j.conbuildmat.2021.125408

Durga, G., Kalra, P., Verma, V. K., Wangdi, K., & Mishra, A. (2021). Ionic liquids: From a solvent for polymeric reactions to the monomers for poly (ionic liquids). *Journal of Molecular Liquids*, 335, 116540. doi:10.1016/j.molliq.2021.116540

El-Saftawy, A. A., Elfalaky, A., Ragheb, M. S., & Zakhary, S. G. (2014). Electron beam induced surface modifications of PET film. *Radiation Physics and Chemistry*, 102, 96 - 102. doi:10.1016/j.radphyschem.2014.04.025

Fang, J., Zhang, L., Sutton, D., Wang, X., & Lin, T. (2012). Needleless melt-electrospinning of polypropylene nanofibres. *Journal of Nanomaterials*, 2012, 382639. doi:10.1155/2012/382639

Francis, R. (2016). *Recycling of Polymers: Methods, Characterization and Applications*. Weinheim, Germany: Wiley-VCH Verlag GmbH &Co.

Ghosal, K., & Nayak, C. (2022). Recent advances in chemical recycling of polyethylene terephthalate waste into value added products for sustainable coating solutions–hope vs. hype. *Materials Advances*, 3(4), 1974 - 1992. doi:10.1039/D1MA01112J

Grigore, M. E. (2017). Methods of recycling, properties and applications of recycled thermoplastic polymers. *Recycling*, 2(4), 24. doi:10.3390/recycling2040024

Gulmine, J. V, Janissek, P. R., Heise, H. M., & Akcelrud, L. (2002). Polyethylene characterization by FTIR. *Polymer Testing*, 21(5), 557 - 563. doi:10.1016/S0142-9418(01)00124-6

Guyot, A., & Bartholin, M. (1982). Design and properties of polymers as materials for fine chemistry. *Progress in Polymer Science*, 8(3), 277 - 331. doi:10.1016/0079-6700(82)90002-8

Hamad, K., Kaseem, M., & Deri, F. (2013). Recycling of waste from polymer materials: An overview of the recent works. *Polymer Degradation and Stability*, 98(12), 2801 - 2812. doi:10.1016/j.polymdegradstab.2013.09.025

Hejna, A., Korol, J., Przybysz-Romatowska, M., Zedler, Ł., Chmielnicki, B., & Formela, K. (2020). Waste tire rubber as low-cost and environmentally-friendly modifier in thermoset polymers–A review. *Waste Management*, 108, 106 - 118. doi:10.1016/j.wasman.2020.04.032

Ignatyev, I. A., Thielemans, W., & Vander Beke, B. (2014). Recycling of polymers: A review. *ChemSusChem*, 7(6), 1579–1593. doi:10.1002/cssc.201300898

Kaur, B., Thakur, N., & Goswami, M. (2023). FTIR spectroscopy based identification and compatibility studies of Gamma Oryzanol with various polymers. *Materials Today: Proceedings*, in press. doi:10.1016/j.matpr.2023.01.164

Khadzhiev, S. N., Kulikova, M. V, Ivantsov, M. I., Zemtsov, L. M., Karpacheva, G. P., Muratov, D. G., Bondarenko, G. N., & Oknina, N. V. (2016). Fischer–Tropsch synthesis in the presence of nanosized iron-polymer catalysts in a fixed-bed reactor. *Petroleum Chemistry*, 56(6), 522 - 528. doi:10.1134/S0965544116060049

Khanam, P. N., & AlMaadeed, M. A. A. (2015). Processing and characterization of polyethylene-based composites. *Advanced Manufacturing: Polymer & Composites Science*, 1(2), 63 - 79. doi:10.1179/2055035915Y.0000000002

Kumar, R. (2021). Tertiary and quaternary recycling of thermoplastics by additive manufacturing approach for thermal sustainability. *Materials Today: Proceedings*, 37, 2382 - 2386. doi:10.1016/j.matpr.2020.08.183

Michell, R. M., & Müller, A. J. (2016). Confined crystallization of polymeric materials. *Progress in Polymer Science*, 54, 183 - 213. doi:10.1016/j.progpolymsci.2015.10.007

Ng, H. M., Saidi, N. M., Omar, F. S., Ramesh, K., Ramesh, S., & Bashir, S. (2018). Thermogravimetric Analysis of Polymers. *Encyclopedia of Polymer Science and Technology* (Ed.) (pp. 1-29). Wiley Online Library. doi:10.1002/0471440264.pst667

Okan, M., Aydin, H. M., & Barsbay, M. (2019). Current approaches to waste polymer utilization and minimization: a review. *Journal of Chemical Technology & Biotechnology*, 94(1), 8 - 21. doi:10.1002/jctb.5778

Özsin, G., & Pütün, A. E. (2018). A comparative study on co-pyrolysis of lignocellulosic biomass with polyethylene terephthalate, polystyrene, and polyvinyl chloride: Synergistic effects and product characteristics. *Journal of Cleaner Production*, 205, 1127 - 1138. doi:10.1016/j.jclepro.2018.09.134

Özsin, G., Kılıç, M., Apaydin-Varol, E., Pütün, A. E., & Pütün, E. (2020). A thermo-kinetic study on co-pyrolysis of oil shale and polyethylene terephthalate using TGA/FT-IR. *Korean Journal of Chemical Engineering*, 37, 1888 - 1898. doi:10.1007/s11814-020-0614-2

Paci, M., & La Mantia, F. P. (1999). Influence of small amounts of polyvinylchloride on the recycling of polyethyleneterephthalate. *Polymer Degradation and Stability*, 63(1), 11 - 14. doi:10.1016/S0141-3910(98)00053-6

Padhan, R. K., & Gupta, A. A. (2018). Preparation and evaluation of waste PET derived polyurethane polymer modified bitumen through in situ polymerization reaction. *Construction and Building Materials*, 158, 337 - 345. doi:10.1016/j.conbuildmat.2017.09.147

Pan, D., Su, F., Liu, H., Liu, C., Umar, A., Castañeda, L., …, & Guo, Z. (2021). Research progress on catalytic pyrolysis and reuse of waste plastics and petroleum sludge. *ES Materials & Manufacturing*, 11(6), 3 - 15. doi:10.30919/esmm5f415

Phakedi, D., Ude, A. U., & Oladijo, P. O. (2021). Co-pyrolysis of polymer waste and carbon-based matter as an alternative for waste management in the developing world. *Journal of Analytical and Applied Pyrolysis*, 155, 105077. doi:10.1016/j.jaap.2021.105077

Picuno, C., Alassali, A., Sundermann, M., Godosi, Z., Picuno, P., & Kuchta, K. (2020). Decontamination and recycling of agrochemical plastic packaging waste. *Journal of Hazardous Materials*, 381, 120965. doi:10.1016/j.jhazmat.2019.120965

Prime, R. B., Bair, H. E., Vyazovkin, S., Gallagher, P. K., & Riga, A. (2009). Thermogravimetric Analysis (TGA). In J. D. Menczel, & R. B. Prime (Eds.), *Thermal Analysis of Polymers: Fundamentals and Applications*, (pp. 241-317). Hoboken, N.J, USA: John Wiley & Sons. doi:10.1002/9780470423837.ch3

Ragaert, K., Delva, L., & Van Geem, K. (2017). Mechanical and chemical recycling of solid plastic waste. *Waste Management*, 69, 24 - 58. doi:10.1016/j.wasman.2017.07.044

Raheem, A. B., Noor, Z. Z., Hassan, A., Abd Hamid, M. K., Samsudin, S. A., & Sabeen, A. H. (2019). Current developments in chemical recycling of post-consumer polyethylene terephthalate wastes for new materials production: A review. *Journal of Cleaner Production*, 225, 1052 - 1064. doi:10.1016/j.jclepro.2019.04.019

Rajasekaran, D., & Maji, P. K. (2018). Recycling of plastic wastes with poly (ethylene-co-methacrylic acid) copolymer as compatibilizer and their conversion into high-end product. *Waste Management*, 74, 135 - 143. doi:10.1016/j.wasman.2018.01.018

Ramarad, S., Khalid, M., Ratnam, C. T., Chuah, A. L., & Rashmi, W. (2015). Waste tire rubber in polymer blends: A review on the evolution, properties and future. *Progress in Materials Science*, 72, 100 - 140. doi:10.1016/j.pmatsci.2015.02.004

Riaz, U., & Ashraf, S. M. (2014). Characterization of Polymer Blends with FTIR Spectroscopy. In S. Thomas, Y. Grohens, & P. Jyotishkumar (Eds.), *Characterization of Polymer Blends*, (pp. 625-678). Weinheim, Germany: Wiley-VCH Verlag GmbH. doi:10.1002/9783527645602.ch20

Saleem, J., Riaz, M. A., & Gordon, M. (2018). Oil sorbents from plastic wastes and polymers: A review. *Journal of Hazardous Materials*, 341, 424 - 437. doi:10.1016/j.jhazmat.2017.07.072

Sharma, R., Joshi, H., & Jain, P. (2011). Short review on the crystallization behavior of PET/clay nanocomposites. *Journal of Chemical Engineering and Materials Science*, 2, 39 - 43.

Singh, N., Hui, D., Singh, R., Ahuja, I. P. S., Feo, L., & Fraternali, F. (2017). Recycling of plastic solid waste: A state of art review and future applications. *Composites Part B: Engineering*, 115, 409 - 422.doi:10.1016/j.compositesb.2016.09.013

Siwal, S. S., Zhang, Q., Devi, N., Saini, A. K., Saini, V., Pareek, B., Gaidukovs, S., & Thakur, V. K. (2021). Recovery processes of sustainable energy using different biomass and wastes. *Renewable and Sustainable Energy Reviews*, 150, 111483. doi:10.1016/j.rser.2021.111483

Srinivasan, S., Valsadwala, A. S., Begum, S. S., & Samui, A. B. (2021). Experimental investigation on the influence of novel catalyst in co-pyrolysis of polymeric waste: Characterization of oil and preparation of char reinforced composites. *Journal of Cleaner Production*, 316, 128225. doi:10.1016/j.jclepro.2021.128225

Suhaimi, N. A. S., Muhamad, F., Abd Razak, N. A., & Zeimaran, E. (2022). Recycling of polyethylene terephthalate wastes: A review of technologies, routes, and applications. *Polymer Engineering & Science*, 62(8), 2355 - 2375. doi:10.1002/pen.26017

Tayyar, A. E., & Üstün, S. (2010). Usage of recycled PET. *Pamukkale University Journal of Engineering Sciences*, 16(1), 53 - 62.

Tonetto, M. R., Pinto, S. C. S., Rastelli, A. de N. S., Borges, A. H., Saad, J. R. C., Pedro, F. L. M., Andrade, M. F. de, & Bandéca, M. C. (2013). Degree of conversion of polymer-matrix composite assessed by FTIR analysis. *Journal of Contemporary Dental Practice*, 14(1), 76 - 79. doi:10.5005/jp-journals-10024-1274

Tsai, T., Laio, J., & Naveen, B. (2015). Preparation and characterization of PET/LDH or clay nanocomposites through the microcompounding process. *Journal of the Chinese Chemical Society*, 62(6), 547–553. doi:10.1002/jccs.201400501

Tufan, M., Gulec, T., Çukur, U., Akbaş, S., & İmamoğlu, S. (2015). Some properties of wood plastic composites produced from waste cups. *Kastamonu University Journal of Forestry Faculty*, 15(2), 176-182.

Valerio, O., Muthuraj, R., & Codou, A. (2020). Strategies for polymer to polymer recycling from waste: Current trends and opportunities for improving the circular economy of polymers in South America. *Current Opinion in Green and Sustainable Chemistry*, 25, 100381. doi:10.1016/j.cogsc.2020.100381

Verdurmen-Noel, L., Baldo, L., & Bremmers, S. (2001). SEC–FTIR characterization of semi-crystalline HDPE and PP. *Polymer*, 42(13), 5523 - 5529. doi:10.1016/S0032-3861(00)00620-0

Woo, E. M., Sun, Y.-S., & Yang, C.-P. (2001). Polymorphism, thermal behavior, and crystal stability in syndiotactic polystyrene vs. its miscible blends. *Progress in Polymer Science*, 26(6), 945 - 983. doi:10.1016/S0079-6700(01)00010-7

Yuan, M., Hu, M., Dai, F., Fan, Y., Deng, Z., Deng, H., & Cheng, Y. (2021). Application of synthetic and natural polymers in surgical mesh for pelvic floor reconstruction. *Materials & Design*, 209, 109984. doi:10.1016/j.matdes.2021.109984

Zhuang, C.-H., Huangfu, W.-H., You, F., Wang, W., Zhu, Y.-S., & Fu, Z.-L. (2022). Evolution and mechanisms of low-temperature oxidation and coal–oxygen coupling processes of a specific low-rank bituminous coal with various microscale particle sizes. *International Journal of Coal Preparation and Utilization*, 43(2), 1 - 21. doi:10.1080/19392699.2022.2051010